



**Financial applications of blockchains and distributed ledgers:  
Group 13, Advanced Portfolio Construction**

---

**Valentin Aolaritei - 368867  
Jérôme Barras - 326256  
Eliot Goncalves - 330553  
Alexandre Joliat - 301765  
Ahmad Mahdavi - 273815**

October 31, 2025

## Part 1

### 1.a

In order to determine our choice of return (either linear or logarithmic) we first performed a qualitative, visual analysis of the marginal distributions for all 14 assets, with both linear and logarithmic daily returns (see Figure 1).

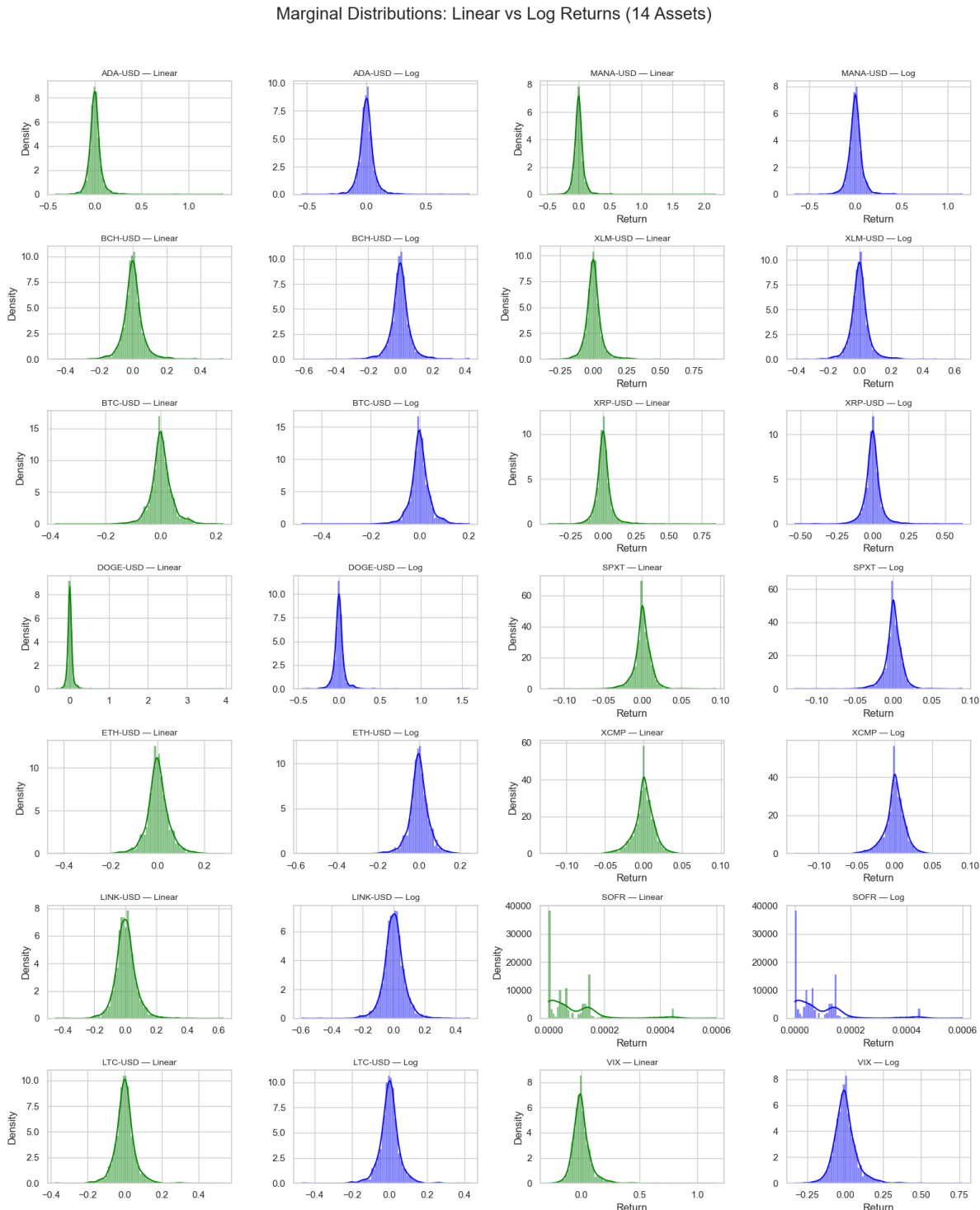


Figure 1: Marginal Distributions of Daily Linear vs Log Returns for All 14 Assets (Linear | Log )

While the images are scaled down and make it difficult to visually detect tail differences in detail, the horizontal axis clearly shows that the linear return distributions stretch to significantly more **extreme values**. As a result, the central mass of the linear return distributions appears **narrower**, indicating heavier tails. These observations suggest meaningful differences in the degree of normality between the distributions of linear and log returns.

To obtain more precise and quantitative insights, we computed key descriptive statistics for both return types, summarized in the tables below.

Table 1: Descriptive Statistics of Daily Linear Returns

Asset	Min	Mean	Max	Median	Skew	Kurtosis
DOGE-USD	-0.3814	0.0048	3.9230	-0.0005	22.3783	838.7119
BCH-USD	-0.5612	0.0023	2.0003	-0.0003	7.6635	193.9386
MANA-USD	-0.4814	0.0045	2.1844	0.0000	7.4611	146.7495
ADA-USD	-0.4166	0.0034	1.3681	0.0000	4.8800	76.2020
VIX	-0.2816	0.0026	1.1560	0.0000	3.5657	37.2509
XLM-USD	-0.3364	0.0030	0.9149	0.0002	3.2998	34.4012
XRP-USD	-0.4162	0.0027	0.8558	0.0003	3.0184	32.5788
SOFR	0.0000	0.0001	0.0006	0.0000	2.4820	7.0413
LINK-USD	-0.4461	0.0034	0.6270	0.0011	0.8453	8.1295
LTC-USD	-0.3726	0.0015	0.5313	0.0006	0.8394	10.8927

Table 2: Descriptive Statistics of Daily Log Returns

Asset	Min	Mean	Max	Median	Skew	Kurtosis
DOGE-USD	-0.4804	0.0019	1.5939	-0.0005	5.0648	106.2563
SOFR	0.0000	0.0001	0.0006	0.0000	2.4815	7.0386
MANA-USD	-0.6565	0.0010	1.1583	0.0000	1.8733	30.5917
VIX	-0.3307	0.0003	0.7682	0.0000	1.8388	14.6091
ADA-USD	-0.5389	0.0012	0.8621	0.0000	1.7722	24.4679
XLM-USD	-0.4101	0.0011	0.6497	0.0002	1.5597	16.4606
XRP-USD	-0.5382	0.0009	0.6183	0.0003	1.1648	18.6759
BCH-USD	-0.8238	-0.0001	1.0987	-0.0003	1.0274	41.6616
LINK-USD	-0.5908	0.0013	0.4867	0.0011	-0.0257	7.1948
LTC-USD	-0.4662	0.0002	0.4261	0.0006	-0.0527	9.6341

The descriptive statistics strongly support the use of log returns for exploratory analysis. On average, crypto assets exhibit much lower skewness and kurtosis when log returns are used: mean skewness drops from **5.01** (linear) to **1.07** (log), and mean kurtosis falls from an extreme **135.53** to a more manageable **27.93**. This reduction in asymmetry and tail thickness makes log returns statistically more stable and closer to normality, which facilitates the estimation of key quantities (e.g., covariance matrix) used in portfolio construction.

The research paper by Meucci (2010, Linear and Compound Return [8]) underlines the fact that the use of linear or log returns has to be a thoughtful choice since one or the other could cause false results. The paper explains that, when projecting the mean or covariance matrix to a longer time horizon, the use of compounded (log) returns can lead to inconsistencies when used for multi-period projections. In our case, we only use the single-period return and do not try to project mean or covariance in the future. Thus, we decided to **pursue the EDA as well as the portfolio construction using log returns** because of their higher normality compared to linear returns.

## 1.b

To identify the presence of unwanted outliers, we began by analyzing the number of values located in the tails of the return distributions. It appeared that a significant number of observations exceeded even  $5\sigma$  (Table 3).

Asset	Total Obs	$> 3\sigma$ Count	$> 4\sigma$ Count	$> 5\sigma$ Count
ADA_USD	1949	33	12	4
BCH_USD	1949	36	18	7
BTC_USD	1949	25	8	2
DOGE_USD	1949	25	10	8
ETH_USD	1949	27	7	2
LINK_USD	1949	29	9	4
LTC_USD	1949	24	11	5
MANA_USD	1949	28	14	7
XLM_USD	1949	33	14	9
XRP_USD	1949	33	16	11
SPXT	1949	28	12	8
XCMP	1949	23	8	5
SOFR	1949	82	13	0
VIX	1949	23	13	5

Table 3: Number of extreme return observations per asset beyond  $3\sigma$ ,  $4\sigma$ , and  $5\sigma$  thresholds.

To further examine the impact of the identified outliers in crypto asset returns, we compared the distribution of raw returns with the distribution after Winsorization. Figures 2 & 3 show boxplots and kernel density estimates (KDE) for each asset, both before and after Winsorization.

In the raw distribution (Figure 2), extreme values and heavy tails are evident in many assets, as seen from the isolated data points and sharp KDE peaks. The Winsorized distribution (Figure 3) caps extreme returns at the 1st and 99th percentiles, which visibly reduces the influence of outliers and makes the return distributions more reasonably normal and less skewed. As a result, the KDE curves are smoother and display significantly less skewness.

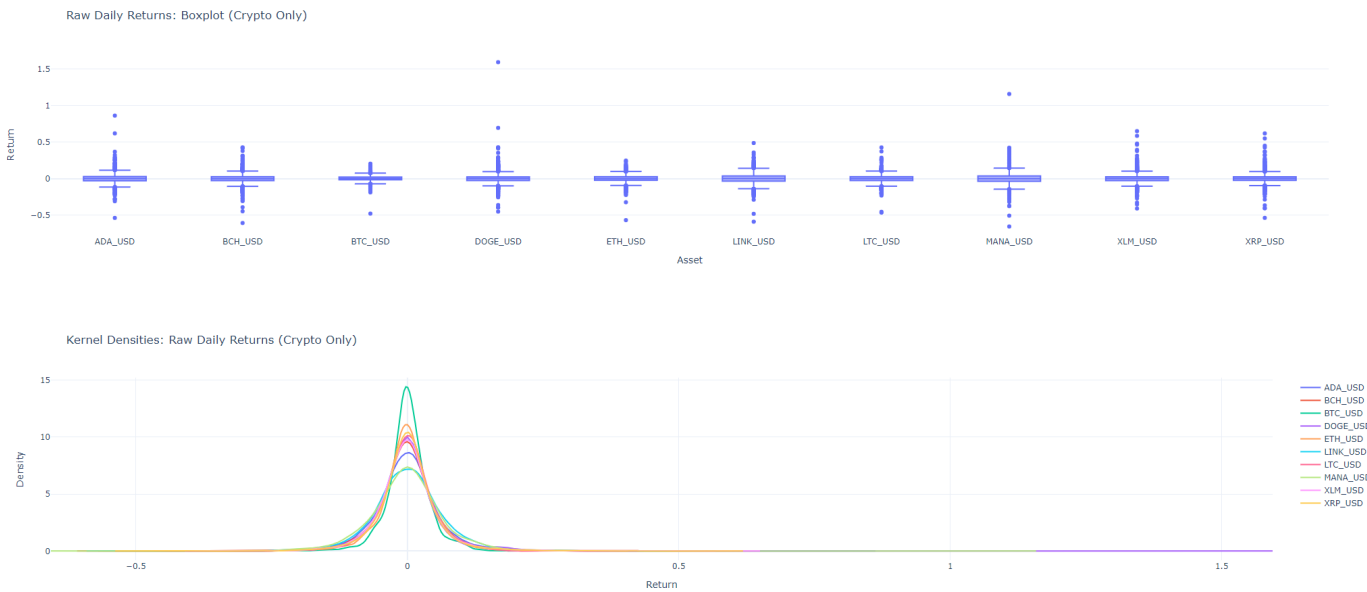


Figure 2: Raw distribution of crypto returns

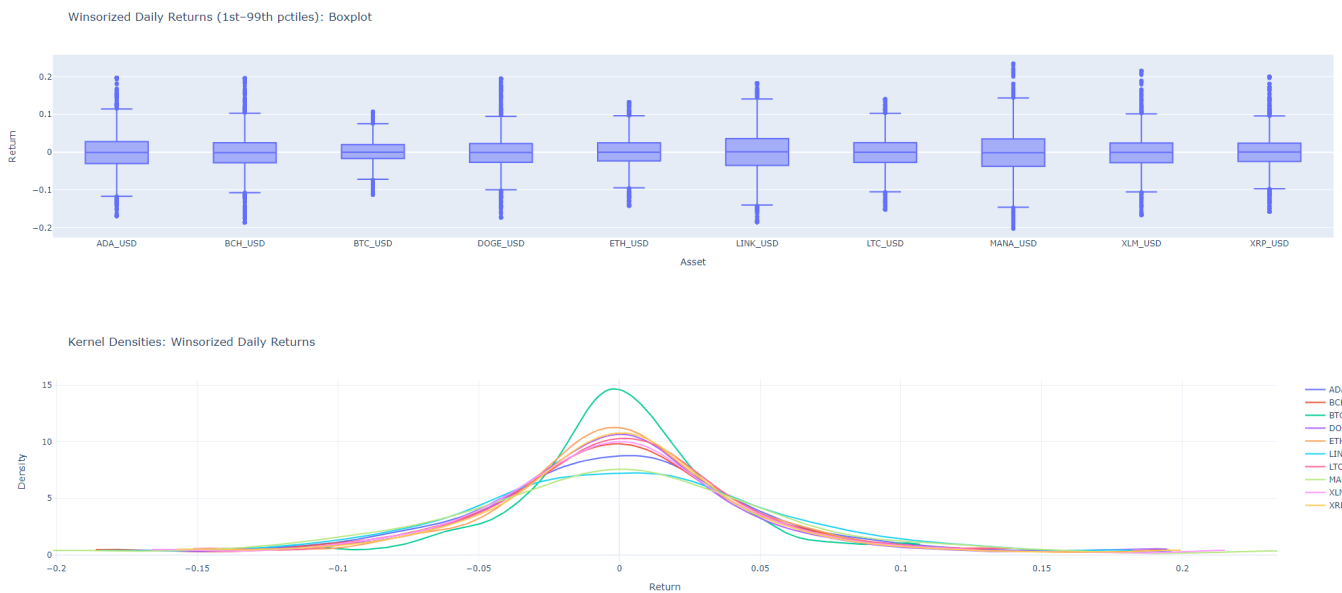


Figure 3: Winsorized distribution of crypto returns

Thus, following insights given in the Möbius guest lecture, we decided to proceed with a cleaned dataset in which these (rare) occurrences of extreme returns were addressed using a **1st and 99th percentile Winsorization**, in order to focus solely on the “normal” behavior of these assets (since it was explained during the same lecture that those extreme returns are symptomatic of the early stage of a crypto and tend to disappear as time goes by).

### 1.c

When evaluating equity indices, using the total-return (TR) versions of SPXT and XCMP rather than their price-return (PR) counterparts matters both in general and for risk-based portfolio optimizations. TR indices take into account the payment of dividends and generally assume that all dividends are reinvested, whereas PR indices ignore them over long horizons. Reinvested dividends have historically accounted for the majority of equity wealth creation, contributing up to 85% of the S&P500’s cumulative return since 1960<sup>9</sup>)

Including dividends also alters the volatility, correlation, and mean structure of returns, since dividend payouts introduce variability in timing and amount with their additional nonzero-sum cash flow component.

For risk-based portfolio optimizations, minimum variance, equal risk contribution, minimum effective number of bets, and hierarchical risk parity, the mean vector and/or covariance matrix of returns serve as key model inputs. Using price return (PR) data understates expected returns by approximately the average dividend yield (typically 1–3% per annum, depending on the period) and misestimates variances and covariances by excluding dividend-related variability. This can lead to sub-optimal portfolio allocations, particularly in frameworks sensitive to marginal risk contributions.

Another important consideration is that the market typically prices dividend payments as a drop in the asset’s value on the ex-dividend date—reflecting the fact that the dividend cash flow is no longer part of the future stream of expected returns. If dividends are not reinvested in the return series (as in PR indices), these mechanically induced price drops appear as negative returns, even though the investor has, in fact, received compensation in the form of a cash payout. In that sense, using PR data introduces misleading downside movements that distort return and risk measures. For these reasons, it is generally essential to use the total return (TR) versions of equity indices in portfolio construction.

## 1.d

While analyzing the data, we observed clear zero returns for non-crypto assets during weekends, due to the public markets being closed. We considered several approaches to address this issue, each with its own advantages and drawbacks:

- **Keeping the dataset as is, including zero returns on weekends for non-crypto assets.** However, this would have meant dealing with misleading zero returns not based on market behavior but on missing data which would artificially reduce volatility estimates and inflate correlations among non-crypto assets. We therefore ruled out this option.
- **Replacing zero returns with random values drawn from a distribution fitted to historical weekday returns.** This approach would have limited the distortion of volatility, mean and covariance but it would have introduced synthetic data, which could not accurately reflect the true market conditions or dynamics at specific points in time, especially during volatile periods.
- **Dropping all weekend observations.** This is the solution we ultimately adopted. We considered that removing data points was preferable to including or generating artificial ones. One consequence of this decision was the exclusion of the date\_PP observation, which fell on a Saturday. However, this did not pose any significant issues, and we assumed that asset behavior did not change materially between the peak date and its neighboring observations.

## Further Analysis

In order to test the hypothesis presented during the Möbius guest lecture regarding the behavior of crypto assets during crisis and recovery periods, we plotted a sample correlation matrix of the crypto assets during both the crash period and the subsequent recovery phase.

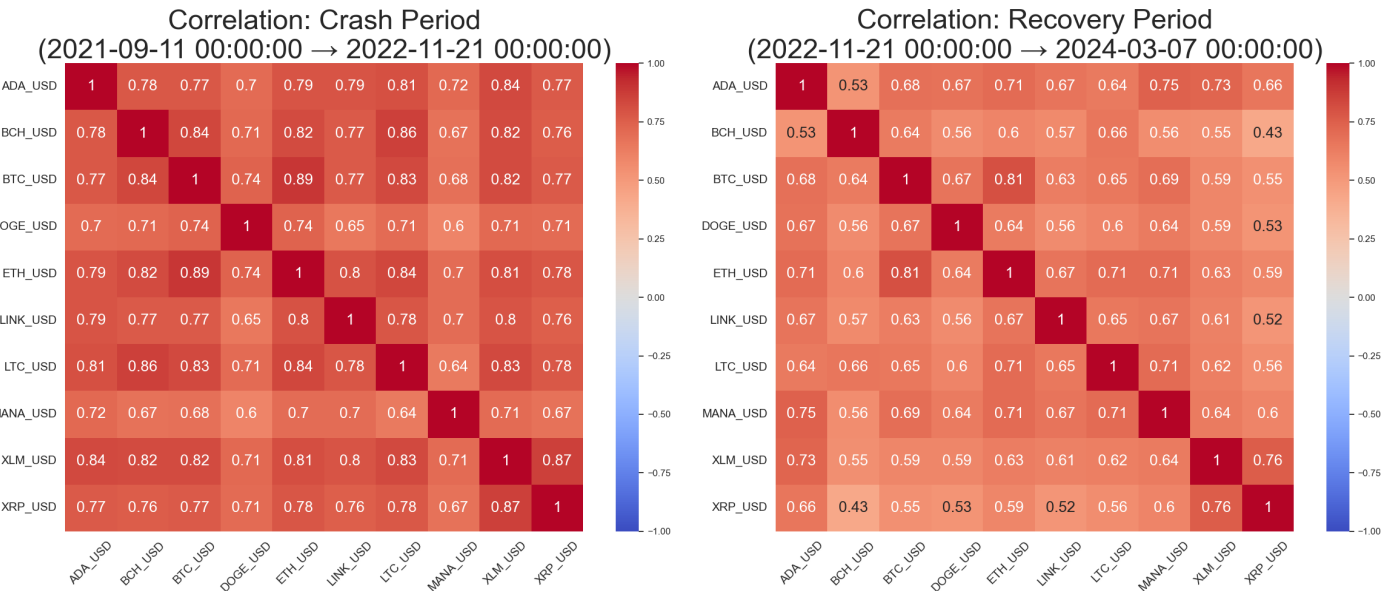


Figure 4: Sample correlation of the crash (left) and recovery (right) periods

We observed a pattern consistent with the insights shared during the Möbius guest lecture: since the COVID-19 crash, crypto assets have increasingly exhibited equity-like behavior. This is particularly evident in the correlation structure during crises, crypto assets tend to move more closely together, resulting in elevated correlations. In contrast, earlier crashes, such as during the early crypto winters, displayed the opposite pattern, with correlations rising during recovery phases.

In our specific analysis of the 2021–2022 crash, we found a clear manifestation of this **equity-like** pattern: rather than seeing higher average correlations during the recovery period, we observed them during the crash itself. Quantitatively, the average pairwise correlation during the crash period was  $\bar{\rho}_{\text{crash}} = 0.763$ , which then dropped to  $\bar{\rho}_{\text{recovery}} = 0.631$  during the recovery phase. This supports the view that the crypto market is maturing and increasingly synchronized with traditional risky-asset behaviors during periods of market stress.

To provide further insight into this correlation dynamic, we plotted the 52-week rolling correlation between Bitcoin and all the other assets. The plot clearly shows a rise in rolling correlations during the crash period, followed by a decline during the recovery:

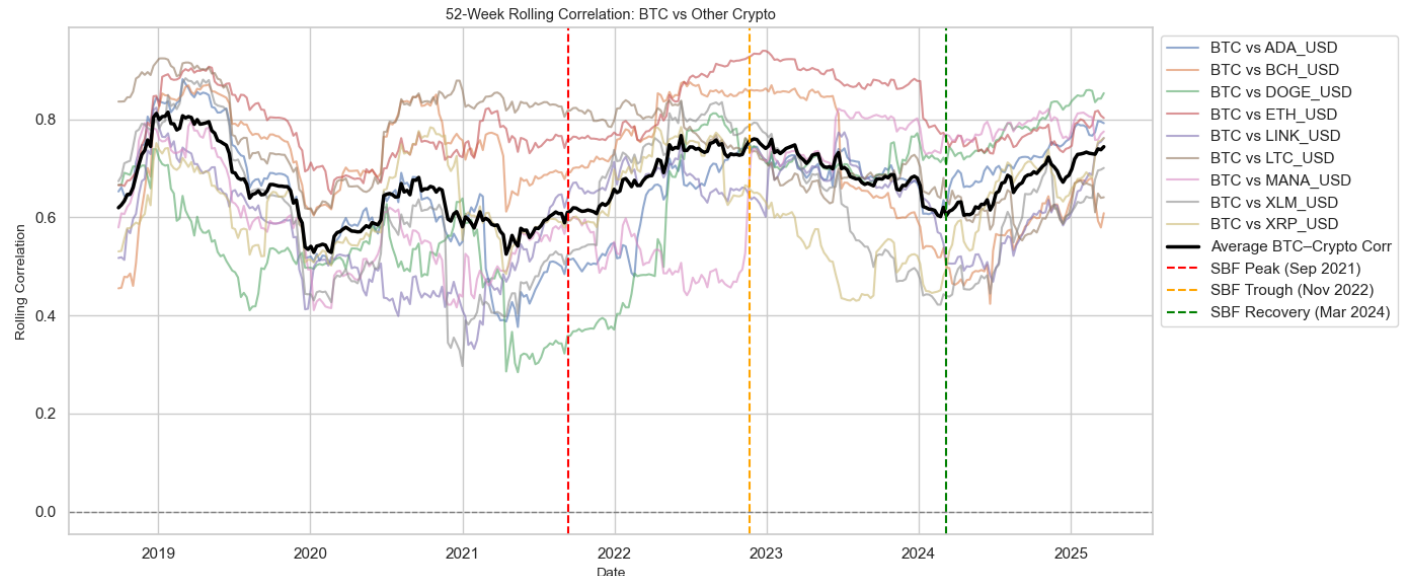


Figure 5: 52-week rolling correlation of BTC vs. all other assets

## Part 2

### a. Equally Weighted Portfolio (EWP)

In this part, an equally weighted portfolio (EWP) is computed for the dates  $datePP$  and  $dateTr$  by applying the formula:

$$\mathbb{E}[R] = \sum_{i=1}^N w_i \cdot \mu_i = \frac{1}{N} \sum_{i=1}^N \mu_i$$

where in the final step we set  $w_i = \frac{1}{N}$ , as all weights must be equal and sum to one. Since we decided to work only with weekdays, we went back to the (winsorized) original dataset for this question, to calculate returns at Peak Date (which is a saturday). With  $N = 14$ , we find that on  $datePP$ , the EWP yields a return of approximately 2%, while on  $dateTr$  it produces a return of -2%. The returns before and after these dates are particularly noteworthy too, especially for  $dateTr$ , as can be observed in *Figure 6*.

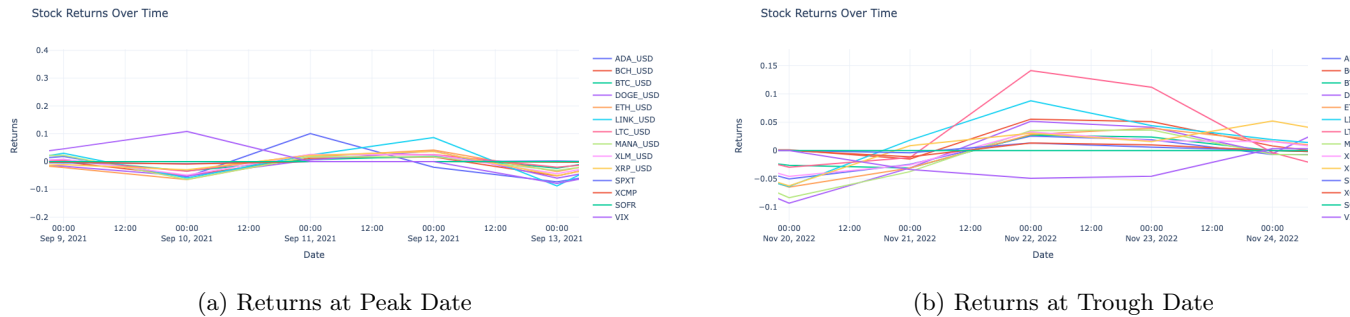


Figure 6: Comparison of Returns at Peak and Trough Dates

### b. Construction of Covariance Matrices

To estimate the sample covariance matrices at each date, we follow the guideline provided in 3, which suggests using at least  $N(N + 1)/2$  observations, where  $N$  is the number of assets. For  $N = 14$ , this implies a minimum of 105 observations, ie 21 weeks of daily data since we removed the week-ends from our dataset. To ensure greater statistical robustness and reduce estimation error, we use a rolling window of 252 daily observations (approximately one trading year). This longer window not only satisfies the minimum data requirement but also smooths out short-term fluctuations and avoids the direct influence of the events occurring around  $dateTr$ , which we believe could distort the covariance estimate.

### c. Covariance Cleaning

To improve the stability of the sample covariance matrix, we apply the eigenvalue clipping method described in [7] to the correlation matrix. This method is motivated by Marčenko–Pastur theory, which shows that in high-dimensional settings (i.e., when the ratio  $q = N/T$  is not close to zero, with  $N$  the number of assets and  $T$  the number of observations), the eigenvalues of the sample covariance matrix are distorted: small eigenvalues are underestimated and large ones are overestimated.

This method involves decomposing the sample correlation matrix into its eigenvalues and eigenvectors; subsequently, all eigenvalues which are smaller than the theoretical Marčenko–Pastur upper edge are replaced by their average. This means that the clipped correlation matrix is

$$\Xi^{\text{clip}} := \sum_{k=1}^N \xi_k^{\text{clip}} \mathbf{u}_k \mathbf{u}_k^*, \quad \xi_k^{\text{clip}} := \begin{cases} \lambda_k & \text{if } \lambda_k \geq \sigma^2(1 + \sqrt{q})^2 \\ \gamma & \text{otherwise} \end{cases}$$

where  $u_k$  are the eigenvectors of the correlation matrix,  $\lambda_k$  are the eigenvalues, and  $\gamma$  is the average of all eigenvalues which are smaller than the upper edge  $\sigma^2(1 + \sqrt{q})^2$ .

After reconstructing the correlation matrix using the clipped eigenvalues and original eigenvectors, we observed that the resulting matrix did not have ones on its diagonal, as is required for a proper correlation matrix. To address this issue, although neither specified nor done in 7, we applied a normalization step: the matrix was rescaled such that its diagonal entries are equal to one. Specifically, let  $\Xi^{\text{clip}}$  denote the cleaned correlation matrix obtained by summing the outer products of the eigenvectors weighted by the clipped eigenvalues. We normalize it as follows:

$$\Xi^{\text{clip}} \leftarrow D^{-1/2} \Xi^{\text{clip}} D^{-1/2}$$

where  $D = \text{diag}(\Xi^{\text{clip}})$  is the diagonal matrix of variances. This ensures that the diagonal of  $\Xi^{\text{clip}}$  is exactly one. Finally, to recover the cleaned covariance matrix, we reintroduce the original standard deviations from the data matrix  $X$  as:

$$\text{Cov}^{\text{clip}} = \Sigma \Xi^{\text{clip}} \Sigma$$

where  $\Sigma = \text{diag}(\sigma_1, \dots, \sigma_N)$  with  $\sigma_i = \sqrt{\text{Var}(X_i)}$  estimated from the sample data. This final matrix,  $\text{Cov}^{\text{clip}}$ , serves as a denoised estimate of the true covariance matrix.

Now, to better understand how these 2 covariance matrices differ, we plotted and analysed a 3D distribution and a kernel density of their respective eigen-spectra for both matrices.

By having a look at *Figure 7*, we can observe that the clipping has achieved its main purpose. In fact, it has reduced noise in the covariance matrix by removing extreme eigenvalues that, in our opinion, likely represented statistical noise rather than true market structure. And so, now the clipped covariance matrix is more stable and can be applied for portfolio optimization purposes.

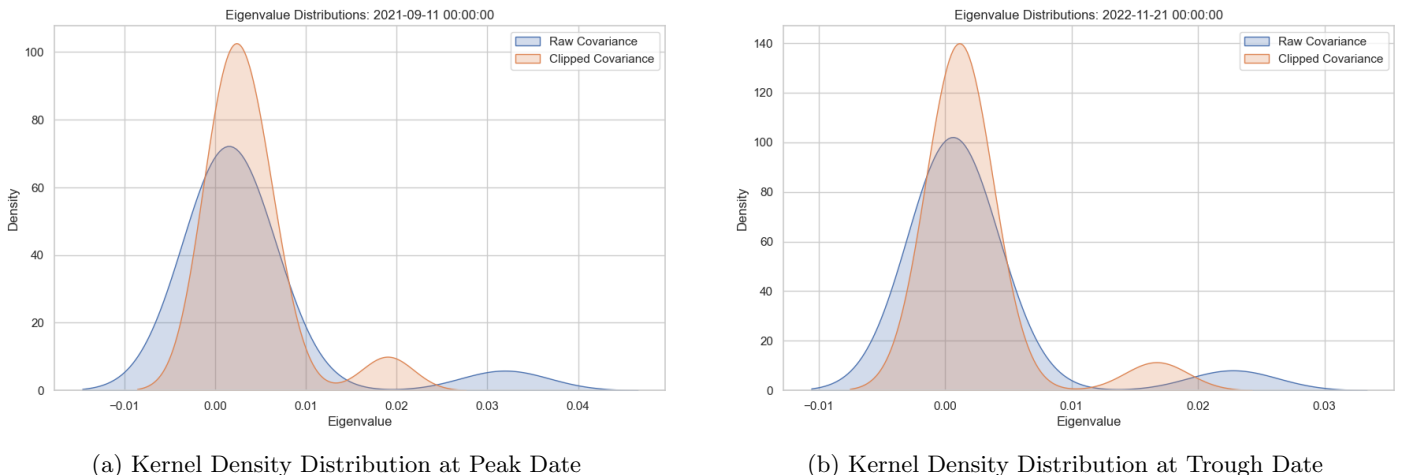


Figure 7: Kernel Density Distributions at Peak and Trough Dates

Now, also by analysing the 3D visualization comparisons in both *Figure 8* and *Figure 9*, it is possible to state that the clipping has achieved its main goal. In both cases, the raw covariance matrix exhibits sharp transitions and large off-diagonal values, indicative of estimation noise present in empirical financial data. In contrast, the clipped matrix preserves the dominant diagonal elements while significantly smoothing the off-diagonal structure.

This shows that the clipping method has effectively reduced the influence of noisy and potentially misleading correlations between assets. By doing so, the cleaned matrix focuses more on the true underlying structure of the data rather than on random fluctuations.

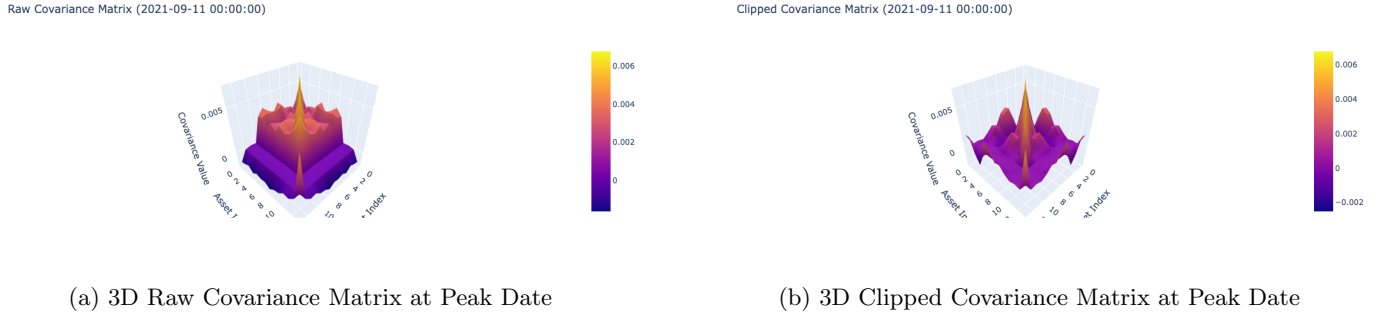


Figure 8: Comparison between 3D Covariance matrices at Peak Dates

Lastly, the condition numbers of the matrices were analysed to provide a mathematical interpretation of this result. Since a covariance matrix is symmetric by definition, we have that:

$$\text{Condition Number} = \frac{\lambda_{\max}}{\lambda_{\min}}$$

where  $\lambda_{\max}$  and  $\lambda_{\min}$  are, respectively, the maximum and minimum eigenvalues of the covariance matrix. This metric is useful because it measures how sensitive the output is to perturbations in the input data and to round-off errors during numerical computations [11]. After computing this value for our four matrices, we observed that the ratio between the condition number of the clipped covariance matrix and that of the raw covariance matrix is:

- $\approx 0.43$  on *datePP*
- $\approx 0.20$  on *dateTr*

This indicates that the clipped covariance matrices are more stable. Therefore, the cleaned covariance matrix is more reliable and better suited for portfolio construction and, for this reason, it will be employed in Part 3 of this project.

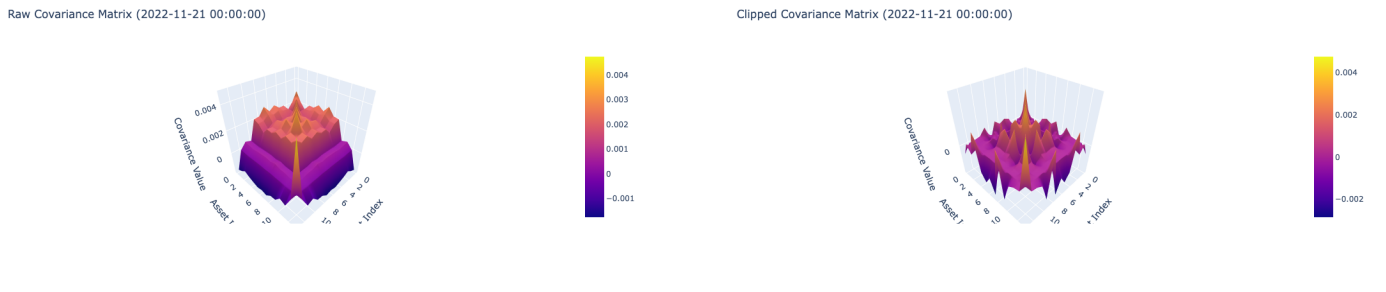


Figure 9: Comparison between 3D Covariance matrices at Trough Dates

#### d. Euler Risk Contribution & Herfindahl-Hirschman index

In this part, the Euler risk contribution for both dates, *datePP* and *dateTr*, and for both matrices, raw and clipped one, was computed. This value indicates how much an asset contributes to the total risk of the portfolio, as stated in [10]. Let's define the risk of the portfolio as

$$\sigma_P = \sqrt{w^T \Sigma w}$$

where  $w$  and  $\Sigma$  indicate, respectively, the weights and the covariance matrix. Since  $\sigma_P$  is homogenous by degree one, we can apply the Euler decomposition. Therefore, we can write

$$\sigma_P = \sum_{i=1}^N w_i \frac{\partial \sigma_P}{\partial w_i} = \sum_{i=1}^N w_i \frac{(\Sigma w)_i}{\sqrt{w^T \Sigma w}} = \sum_{i=1}^N R C_i = w^T \frac{\Sigma w}{\sqrt{w^T \Sigma w}} = \sqrt{w^T \Sigma w} = \sigma_P$$

where  $R C_i$  indicates the Euler risk contribution of each asset.

In order to understand better how each asset contributes to the overall risk, we plotted the percentage of risk contribution for each asset, as can be observed in *Figure 10* and *Figure 11*.

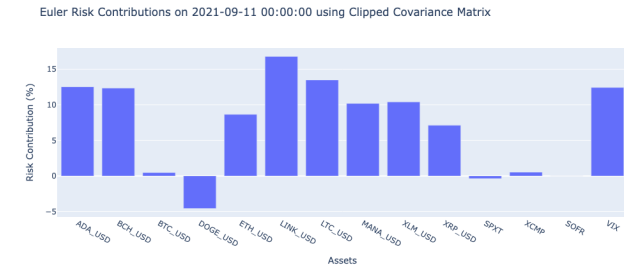
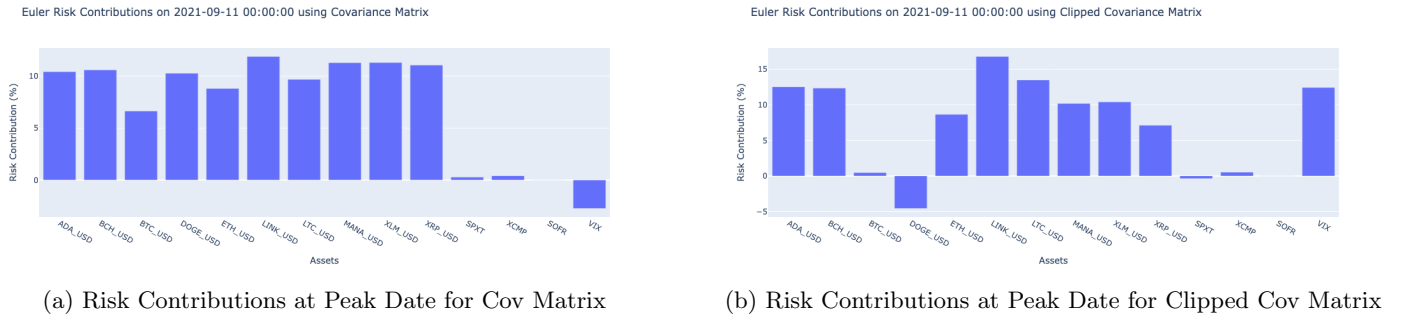


Figure 10: Comparison between Risk Contributions at Peak Date

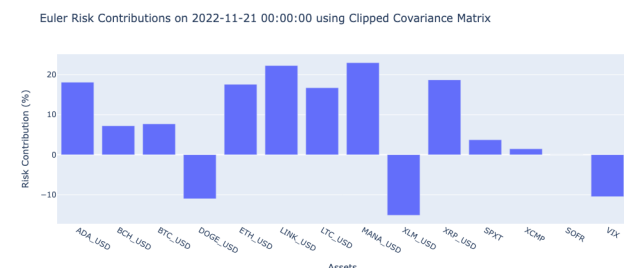
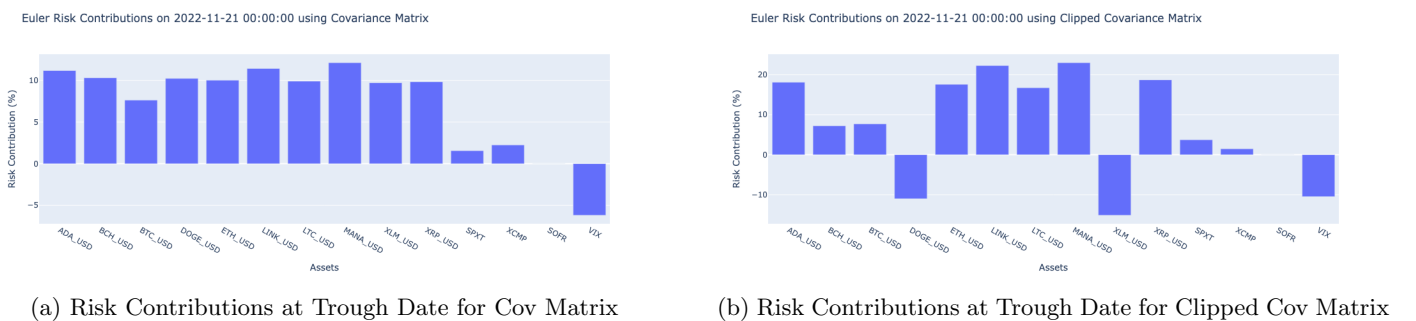


Figure 11: Comparison between Risk Contributions at Trough Date

At a glance, it is interesting to note how the signs stay constant for the raw covariance matrices across the two dates. On the other hand, assets' risk contributions do not always have same sign when using the clipped matrices.

By comparing *Figure 10a* and *Figure 11a*, we can state that the overall distribution just shows changes in magnitude for all components. Notably, VIX's risk contribution turns significantly more negative in the later period, suggesting it acted more as a risk mitigator or hedge in 2022 than in 2021. On the other hand, SPX and XCMP slightly increased, indicating that volatility for traditional assets increased too during that period. By comparing *Figure 10b* and *Figure 11b*, we observe that between September 2021 and November 2022, the risk profile of crypto assets changed significantly. LINK\_USD remained a top risk contributor, while MANA\_USD's impact doubled. DOGE\_USD consistently stayed negative, but XLM\_USD and VIX newly emerged as significant hedges in 2022. Comparing *Figure 10a* and *Figure 10b*, it shows significant differences. With the raw covariance matrix, risk contributions are more evenly distributed across all cryptocurrencies. The clipped covariance matrix reveals more variation in risk, with LINK\_USD showing the highest contribution (16%) and DOGE\_USD becoming a negative contributor (-5%). Moreover, by having a look at *Figure 11*, the raw covariance matrix shows relatively uniform positive risk contributions across most cryptocurrencies, with only the traditional asset VIX providing

meaningful hedging, around  $-6\%$ . The clipped covariance matrix reveals much greater dispersion, with LINK\_USD and MANA\_USD contributing over 20% risk each, while DOGE\_USD, XLM\_USD, and VIX act as significant hedges, with values between  $-10\%$  and  $15\%$ . Overall, we came to the conclusion that the clipping method appears to uncover hedging relationships and risk concentrations that are not visible in the raw calculation.

Overall, the portfolio shows more extreme risk contributions, both positive and negative, in 2022.

After analysing the contribution of each asset to the total risk of the portfolio, we condensed all the Euler risk contribution into a single and unique measure, the Herfindahl-Hirschman index. As stated in 12, it provides a measure of concentration in the risk contribution structure of a portfolio. More precisely, it describes you how evenly or unevenly risk is distributed across the assets in the portfolio. This index is computed as

$$HHI = \sum_{i=1}^N \left( \frac{RC_i}{\sigma_P} \right)^2 = \frac{1}{\sigma_P^2} \sum_{i=1}^N RC_i^2 \in [0, 1]$$

In our case, the results we get can be observed in Table 4

	<i>datePP</i>	<i>dateTr</i>
Raw Covariance matrix	10.7054%	11.08%
Clipped Covariance matrix	12.8779%	28.79%

Table 4: HHI on *datePP* and *dateTr*

So, by comparing the Herfindahl index across raw and cleaned covariance estimators, we can state that the cleaning process concentrates the risk contribution structure. This means that in both cases, risk is more concentrated in fewer assets, which can also be observed from *Figure 10* and *Figure 11*.

### e. Diversification Distribution & Effective Number of Bets

In this section, we compute the diversification distribution as described in [13]. First, let's consider our covariance matrix  $\Sigma$ . We know that

$$\Lambda = E^T \Sigma E$$

where the diagonal matrix  $\Lambda = diag(\lambda_1, \dots, \lambda_N)$  contains the eigenvalues of  $\Sigma$ , sorted in decreasing order, and the columns of the matrix  $E = (e_1, \dots, e_N)$  are the respective eigenvectors. Now, we can define the diversification distribution as

$$p_n = \frac{\tilde{w}^2 \lambda_n}{w^T \Sigma w}$$

where  $\tilde{w} := E^{-1}w$ .

The results can be visualised in Figure 12 and Figure 13

By comparing these results with the ones obtained previously, we can state that at *datePP*, the raw covariance matrix shows concentrated risk in a few crypto assets(majority in ADA\_USD), with limited diversification reflected in the Diversification Distribution. In contrast, Euler Risk Contributions spread risk more evenly by accounting for asset correlations. When using the clipped covariance matrix, both measures become more balanced, as clipping reduces noise and extreme eigenvalues, improving the reliability of risk attribution. A similar pattern appears at *dateTr*: the raw matrix again shows concentrated diversification distribution in ADA\_USD, while clipping leads to a more even distribution.

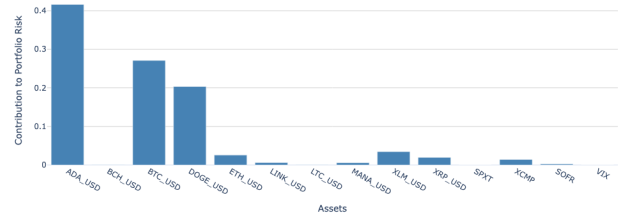
Overall, we believe that the clipping method enhances the stability and interpretability of risk estimates by mitigating distortions from estimation noise.

Diversification Distribution on 2021-09-11 for Raw Cov Matrix



(a) Diversification Distribution at Peak Date for Raw Covariance Matrix

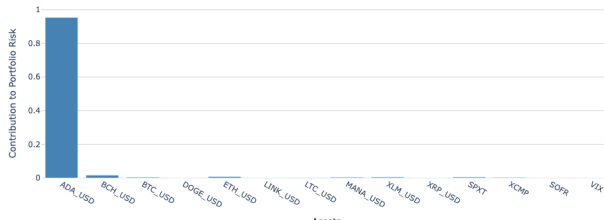
Diversification Distribution on 2021-09-11 for Clipped Cov Matrix



(b) Diversification Distribution at Peak Date for Clipped Covariance Matrix

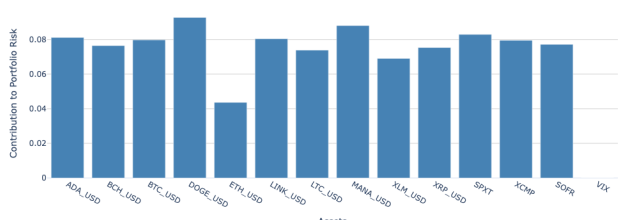
Figure 12: Comparison between Diversification Distributions at Peak Date

Diversification Distribution on 2022-11-21 for Raw Cov Matrix



(a) Diversification Distribution at Trough Date for Raw Covariance Matrix

Diversification Distribution on 2022-11-21 for Clipped Cov Matrix



(b) Diversification Distribution at Trough Date for Clipped Covariance Matrix

Figure 13: Comparison between Diversification Distributions at Trough Date

Now, as done before, we summarized and condensed all the information provided by the diversification distribution into a single value, the effective number of bets(ENB). This value is defined as

$$ENB = e^{-\sum_{i=1}^N d_n \log_e d_n}$$

where  $d_n$  represents the diversification distribution of asset  $n$ . The results we get can be viewed in *Table 5*.

	datePP	dateTr
Raw Covariance matrix	1.142	1.214
Clipped Covariance matrix	2.098	6.499

Table 5: Effective Number of Bets on *datePP* and *dateTr*

By comparing the effective number of bets with the Herfindahl-Hirschman Index, we can state that by using the clipped covariance matrix, the ENB increases, showing that the portfolio appears more diversified due to reduced noise and clearer identification of independent risks. At the same time, the HHI also rises, meaning that risk is less evenly spread among these sources. This means clipping uncovers more distinct risk factors but also reveals that some contribute more heavily than others—something the raw, noisier matrix tends to hide.

## f. Comparison between Euler's Risk and Observed Loss

In order to analyze the relevance of the Euler risk computed in *Part 2d* as an indicator of an asset's propensity to incur losses relative to the other assets in the portfolio, we compared the rank order of the cumulative losses over the period to the rank order of the Euler risk contributions during the same timeframe.

We started by computing the cumulative losses over the period `date_PP` to `date_Tr`, which, due to the additive property of log returns, was simply the sum of daily returns for each asset. This gave us a ranking of the largest losers over the period, as shown in (Figure 14).

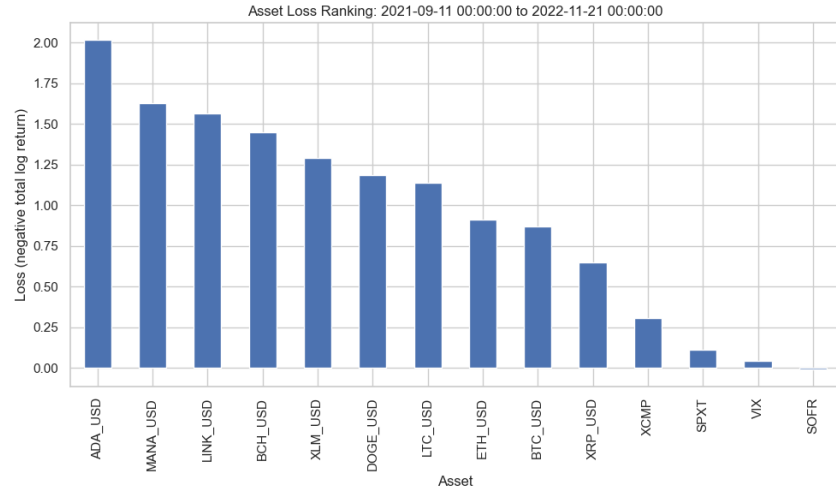


Figure 14: Biggest losers by cumulative negative returns over the period `date_PP` to `date_Tr`

We then combined the cumulative losses and Euler risk contribution percentages (computed in `d`) into a single dataset and plotted the rank order of losses against the rank order of Euler risk contributions in (Figure 15).

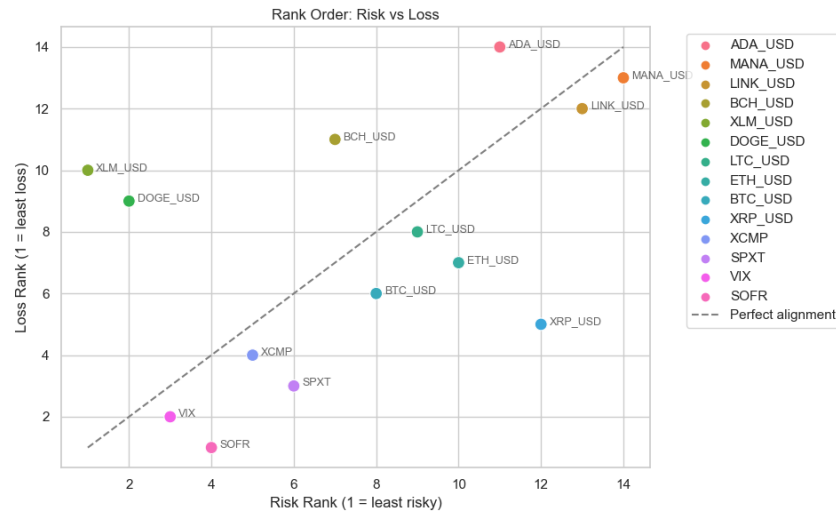


Figure 15: Rank order of cumulative losses vs. rank order of Euler risk contributions for `date_PP` to `date_Tr`

As we can see, there appears to be a clear trend between the rank of the Euler risk and the rank of the observed losses over the period, suggesting that the Euler risk measure captures, to some extent, the assets most at risk. However, the relationship is not perfect, as no single data point lies exactly on the diagonal line that would indicate a perfect correspondence between the two rankings.

To obtain a more quantitative assessment of the relationship between the two rankings, we computed Kendall's tau correlation coefficient, which measures the ordinal association between two variables. This coefficient is accompanied by a p-value for a hypothesis test evaluating the statistical significance of the observed association. We obtained the following results:

$$Kendall_{\tau} = 0.34 \quad | \quad p_{value} = 0.101$$

This result suggests a positive but statistically non-significant correlation between the two rankings at the 10% significance level but it is close to the threshold. Therefore, while Euler risk contributions may provide some insight into the relative riskiness of each asset, they should not be interpreted as fully reliable predictors of losses.

## Part 3

### a: Construction of Risk-Based Portfolios

In this section, we construct four distinct risk-based portfolios as of two key market dates: the previous peak (`datePP` = 11-Sep-2021) and the market trough (`dateTr` = 21-Nov-2022). Each portfolio is computed using the cleaned covariance matrix, obtained via eigenvalue clipping to ensure numerical stability and robust out-of-sample performance. The optimization of portfolio weights is performed under the standard constraints of full investment ( $\sum w_i = 1$ ) and non-negativity ( $w_i \geq 0$ ), i.e., no short-selling or leverage.

#### i. Minimum Variance Portfolio (MVP):

The MVP seeks to minimize the total portfolio variance:

$$\min_w \quad w^\top \Sigma w \quad \text{subject to} \quad \sum w_i = 1, \quad w_i \geq 0$$

This formulation is based on the classical mean-variance framework introduced by Markowitz (1952)<sup>14</sup>, but we exclude the expected return term to focus purely on risk minimization. The MVP typically assigns larger weights to low-volatility and weakly correlated assets, often resulting in concentrated portfolios. As highlighted by Roncalli et al. (2009), the MVP equalizes the marginal risk contributions across assets, which may unintentionally lead to significant concentration in assets like cash or low-risk bonds.

#### ii. Equal Risk Contribution Portfolio (ERC):

The ERC portfolio, also known as the risk parity portfolio, equalizes each asset's total contribution to portfolio risk. If we assume that the standard deviation of the portfolio is a homogeneous function of the weights  $\omega$ , then Euler's theorem for homogeneous functions states that:

$$\sigma(\omega) = \sum_{i=1}^n \omega_i \frac{\partial \sigma(\omega)}{\partial \omega_i} = \sum_{i=1}^n \sigma_i(\omega)$$

i.e., each asset  $i$ , weighted  $\omega_i$ , whose returns are  $r_i$ , makes a contribution to the risk:

$$\sigma_i(\omega) = \omega_i \frac{\partial \sigma(\omega)}{\partial \omega_i} = \omega_i \frac{\omega_i \sigma_{ii} + \sum_{j \neq i} \omega_j \sigma_{ij}}{\sigma(\omega)}$$

$\sigma_i(\omega)$  is called the  $i^{th}$  *risk contribution* for a portfolio  $\Omega : \omega = (\omega_i)_{1 \leq i \leq n}$ .

The goal of this optimization is to find the vector  $\omega$  such that for all  $i \neq j$ ,  $\sigma_i(\omega) = \sigma_j(\omega)$ . Mathematically we can write the problem as the following:

$$\omega^* = \left\{ \omega_k \in [0, 1]^n : \sum_{i=1}^n \omega_i = 1, \quad \omega_i \frac{\partial \sigma(\omega)}{\partial \omega_i} = \omega_j \frac{\partial \sigma(\omega)}{\partial \omega_j} \quad \forall i, j \right\}$$

In our case, we can consider this algorithm as an alternative:<sup>15</sup>

$$y^* = \arg \min_y \sqrt{y^\top \Sigma y} \quad \text{u.c.} \quad \begin{cases} \sum_{i=1}^n \ln y_i \geq c \\ y \geq 0 \end{cases} \quad (7)$$

with  $c$  an arbitrary constant. This algorithm is similar to a variance minimization problem subject to a constraint of sufficient diversification of weights. It can be solved using SLSQP. The Equal Risk Contribution (ERC) portfolio is expressed as:

$$x^* = \frac{y_i^*}{\sum_{i=1}^n y_i^*}$$

### iii. Minimum Effective Number of Bets (ENB):

Inspired by Meucci (2009)<sup>13</sup>, this portfolio minimizes the Effective Number of Bets (ENB), which quantifies true diversification. The ENB is defined as:

$$ENB(w) = \exp \left( - \sum_i p_i \log p_i \right), \quad \text{where } p_i = \frac{(\tilde{w}_i)^2}{\sum_j (\tilde{w}_j)^2}, \quad \tilde{w}_i = w_i \cdot \sigma_i$$

We can approximate this by minimizing  $\sum_i (w_i \cdot \sigma_i)^2$ , which is proportional to the Herfindahl index of scaled weights. This approach yields portfolios that are deliberately concentrated in a small number of dominant, relatively uncorrelated exposures, offering a useful contrast to ERC.

Alternatively, we can compute the ENB<sup>1</sup> portfolio more precisely by maximizing the diversification entropy of the portfolio in the uncorrelated risk-factor space.

The resulting optimization problem is:

$$\min_w - \sum_{i=1}^n d_i \log d_i, \quad \text{s.t.} \quad \sum_{i=1}^n w_i = 1, \quad w_i \in [0, 1]$$

We solve this numerically using Sequential Least Squares Programming (SLSQP), ensuring the usual linear conditions.

### iv. Hierarchical Risk Parity (HRP):

The HRP algorithm, introduced by Lopez de Prado (2016)<sup>3</sup>, provides a robust alternative to traditional risk-based portfolios by avoiding matrix inversion. It comprises three stages:

- (a) **Tree Clustering:** Assets are hierarchically clustered using a distance matrix derived from the correlation matrix:  $d_{ij} = \sqrt{(1 - \rho_{ij})/2}$ .
- (b) **Quasi-Diagonalization:** The assets are reordered based on the dendrogram structure to reflect similarity in risk profiles.
- (c) **Recursive Bisection:** Portfolio weights are allocated recursively by dividing clusters and assigning capital inversely proportional to cluster variances.

The resulting portfolios tend to be well-diversified and less sensitive to estimation error in the covariance matrix. HRP portfolios adapt to the underlying correlation structure and can respond dynamically to shifts in clustering behavior among assets.

Each portfolio construction method reflects a different philosophical stance on risk allocation: MVP emphasizes variance minimization, ERC distributes risk evenly, ENB concentrates exposure into a few orthogonal factors, and HRP balances risk hierarchically based on empirical structure. These differences lead to significantly different weight profiles and diversification properties, which we compare and discuss further in Part 3(b).

<sup>1</sup>Formulas are provided in *Part 2e*

The six studied portfolios weights, both at datePP and dateTr using the clipped covariance matrix are shown as follows:

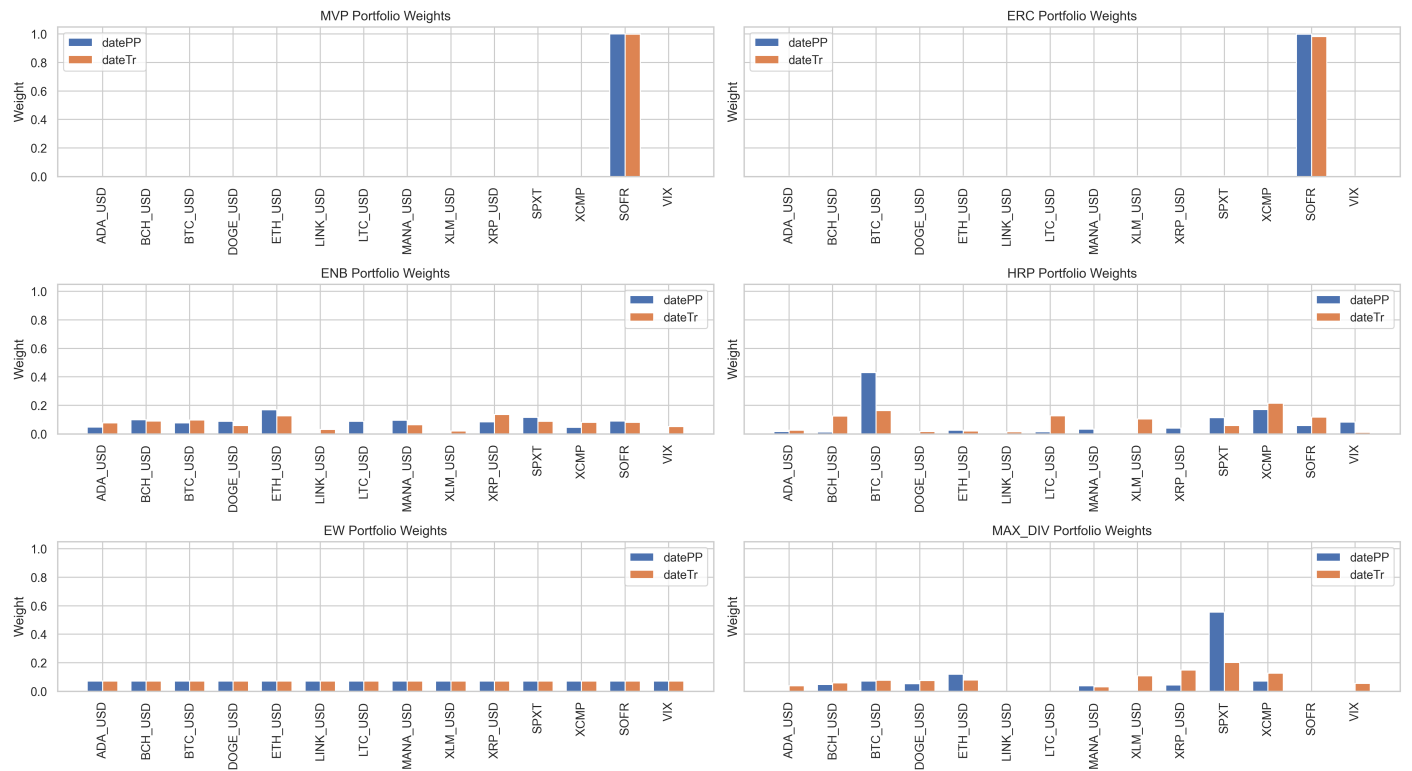


Figure 16: The 6 portfolios weights, both at datePP and dateTr

Portfolio	ADA	BCH	BTC	DOGE	ETH	LINK	LTC	MANA	XLM	XRP	SPXT	XCMP	SOFR	VIX	
<b>MVP_PP</b>	0.0000	0.0000	0.0000	0.0010	0.0000	0.0000	0.0000	0.0000	0.0000	0.0000	0.0000	0.0000	<b>0.9999</b>	0.0000	
<b>ERC_PP</b>	0.0000	0.0000	0.0001	0.0001	0.0001	0.0000	0.0000	0.0000	0.0000	0.0000	0.0001	0.0006	0.0003	<b>0.9986</b>	0.0000
<b>ENB_PP</b>	0.0483	0.0987	0.0762	0.0883	<b>0.1696</b>	0.0000	0.0878	0.0958	0.0000	0.0843	0.1164	0.0454	0.0892	0.0000	
<b>HRP_PP</b>	0.0158	0.0118	<b>0.4296</b>	0.0012	0.0262	0.0000	0.0135	0.0327	0.0043	0.0396	0.1135	0.1707	0.0589	0.0823	
<b>MAXDIV_PP</b>	0.0000	0.0470	0.0713	0.0533	0.1198	0.0000	0.0000	0.0391	0.0000	0.0434	<b>0.5553</b>	0.0708	0.0000	0.0000	
<b>EW_PP</b>	All weights = 0.0714 (uniform)														
<b>MVP_Tr</b>	0.0000	0.0000	0.0000	0.0010	0.0000	0.0000	0.0000	0.0000	0.0010	0.0000	0.0000	0.0000	<b>0.9987</b>	0.0001	
<b>ERC_Tr</b>	0.0007	0.0008	0.0010	0.0014	0.0008	0.0008	0.0009	0.0011	0.0039	0.0013	0.0028	0.0020	<b>0.9815</b>	0.0010	
<b>ENB_Tr</b>	0.0775	0.0892	0.0973	0.0592	0.1266	0.0303	0.0000	0.0642	0.0201	0.1360	0.0876	0.0809	0.0804	0.0508	
<b>HRP_Tr</b>	0.0261	0.1245	0.1631	0.0158	0.0208	0.0151	0.1258	0.0033	0.1051	0.0000	0.0579	0.2153	0.1170	0.0103	
<b>MAXDIV_Tr</b>	0.0381	0.0586	0.0766	0.0751	0.0794	0.0000	0.0000	0.0314	0.1077	0.1493	0.2027	0.1268	0.0000	0.0543	
<b>EW_Tr</b>	All weights = 0.0714 (uniform)														

Table 6: All six Portfolios Weights at both datePP and dateTr

Where the dominant weights were highlighted for each portfolio.

## b. Comparison of Optimal Weights across Time

The following plots show the comparison of all six studied porfolios in part 3.a) across both datePP and dateTr and among each other:

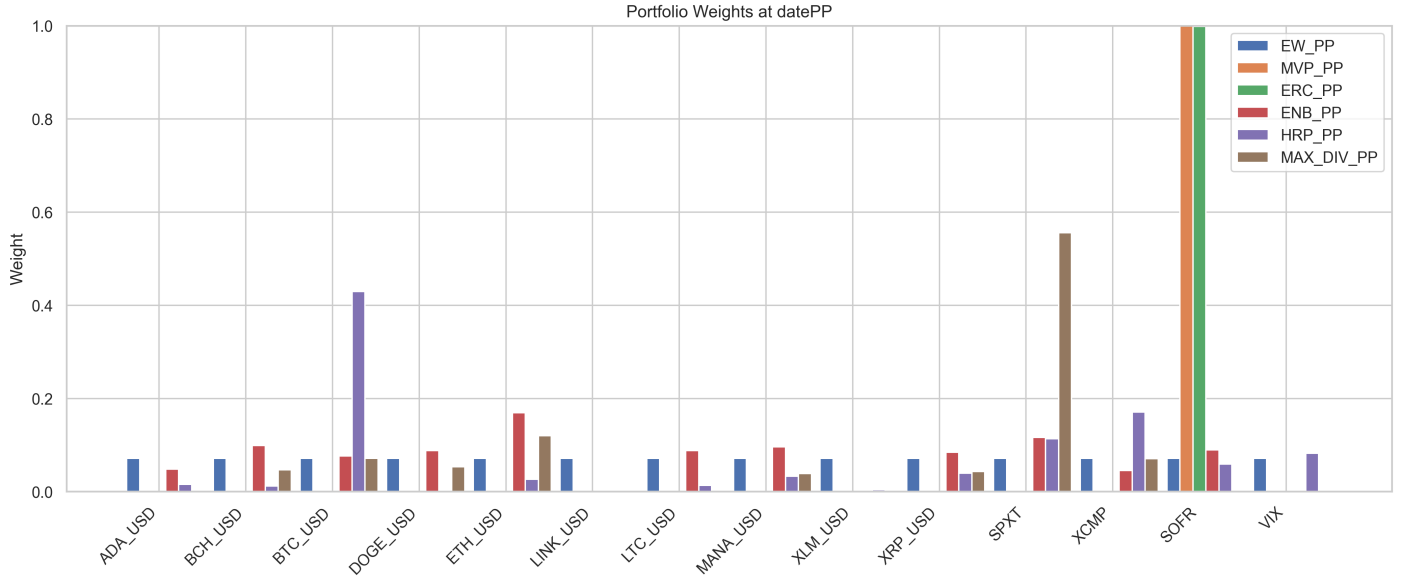


Figure 17: comparison of all six studied portfolios in part 3.a) across datePP and among each other

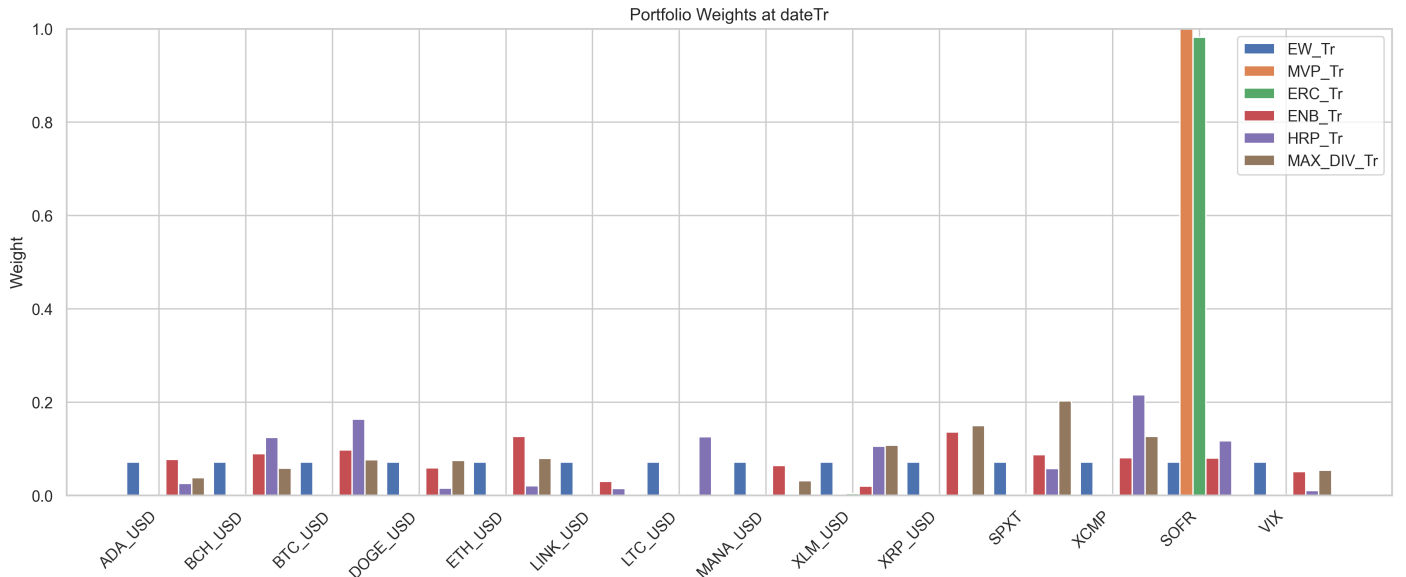


Figure 18: comparison of all six studied portfolios in part 3.a) across dateTr and among each other

The six portfolios exhibit markedly different allocation behaviors across dates and methodologies. Both the Minimum Variance Portfolio (MVP) and the Equal Risk Contribution (ERC) portfolios are highly concentrated in SOFR at both datePP and dateTr, reflecting their preference for minimal volatility and stable risk contribution. MVP, in particular, allocates nearly 99% to SOFR, leaving negligible weights for other assets (Figure 18, Figure 17).

In contrast, the Meucci (ENB) and Hierarchical Risk Parity (HRP) portfolios show significantly greater diversification. ENB distributes weights across a broad mix of crypto and equity assets, with a notable shift from ETH and DOGE at datePP to XRP and ETH at dateTr, demonstrating responsiveness to changes in correlation structure. HRP also adapts to date-specific conditions, reallocating from a BTC-heavy position at datePP to a more balanced exposure including XCMF, BCH, and XLM at dateTr. The Maximum Diversification (MAXDIV) portfolio avoids low-volatility assets like SOFR altogether,

instead favoring high-volatility and low-correlation assets such as SPXT, ETH, and XRP. Finally, the Equal Weight (EW) portfolio provides a constant and naive benchmark, allocating uniformly across all assets regardless of market conditions. Overall, MVP and ERC offer low-risk but impractically concentrated solutions, while ENB, HRP, and MAXDIV yield more balanced portfolios that reflect structural differences in asset interactions over time.

The following table summarizes these observations :

Portfolio	Concentration	Most Favored Asset(s)	Diversification	Style / Assumption
<b>MVP</b>	Very high	SOFR	Very low	Volatility minimizer
<b>ERC</b>	Very high	SOFR	Low	Equal risk share
<b>ENB</b>	Moderate	ETH, DOGE, BCH, XRP	High	Energy minimization
<b>HRP</b>	Moderate	BTC, XCMP, BCH	Medium-high	Tree-based, cluster-aware
<b>MAXDIV</b>	Moderate	SPXT, ETH, XRP	Medium	Diversification ratio maximizer
<b>EW</b>	None	All equally	Maximum (naive)	Benchmark only

Table 7: Comparison of Portfolio Characteristics Across Methods

The following plots relate the risk contribution found in part 2 and the weights of each six portfolios, both for datePP and dateTr :

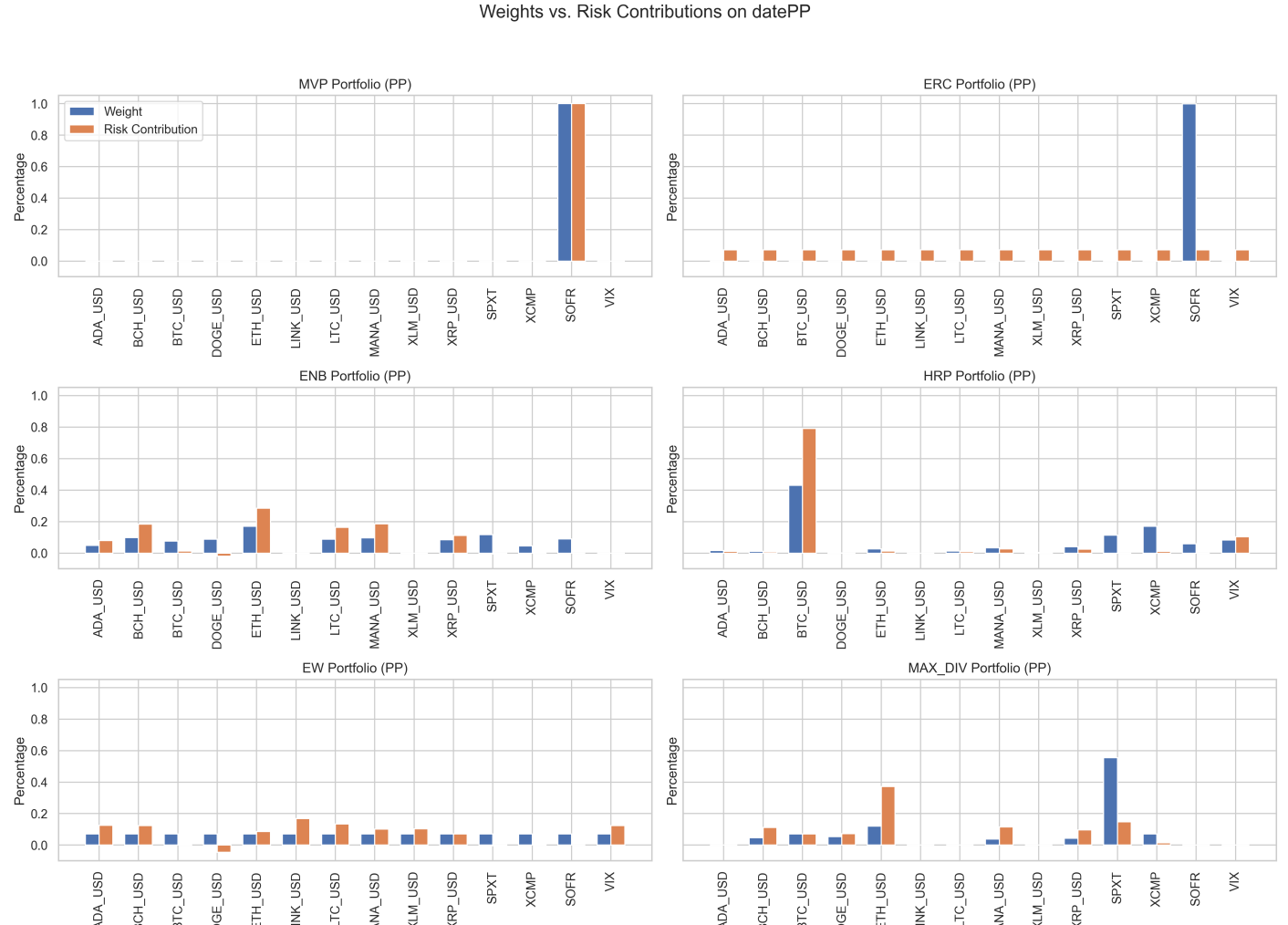


Figure 19: Weights vs. risks contributions on datePP

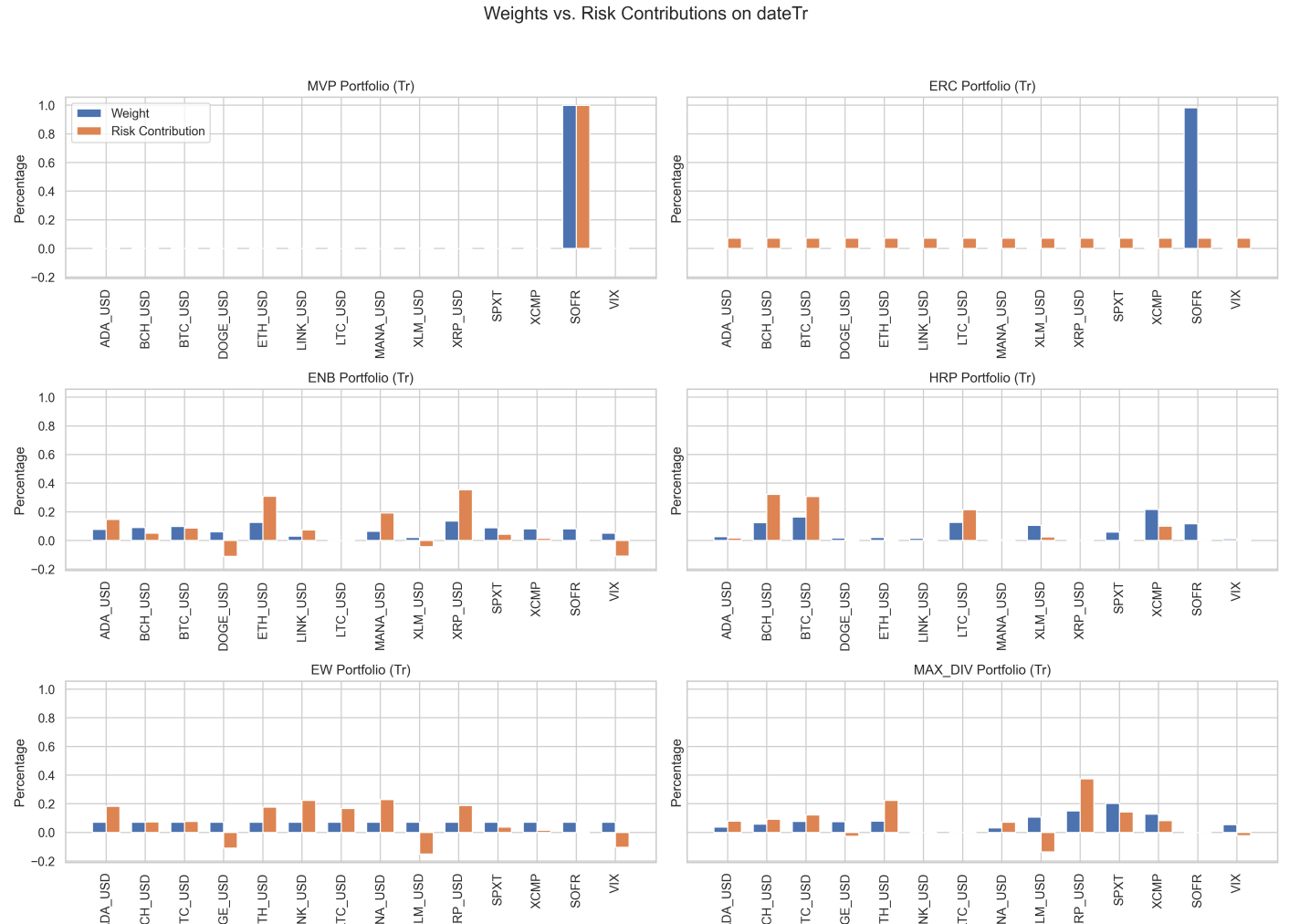


Figure 20: Weights vs. risks contributions on dateTr

As shown in Figure 19, 20, we can see that the comparison between weights and risk contributions reveals important differences in how each portfolio construction method handles risk allocation, particularly under changing market conditions.

At datePP, both the MVP and ERC portfolios show extreme concentration in SOFR, with nearly all portfolio weight allocated to this low-volatility asset. However, despite this, risk is much more evenly distributed across all assets. This occurs because the few percent of weight allocated to high-volatility crypto assets contribute disproportionately to total portfolio risk. This demonstrates a key insight: minimizing variance or equalizing risk does not imply uniform risk contributions when assets have drastically different volatilities.

The HRP and ENB portfolios offer more balanced weight allocations and, as shown in the charts, their risk contributions better align with their weights. HRP at datePP, for example, gives over 40% weight to BTC, but its risk contribution is significantly higher — reflecting BTC’s high volatility. At dateTr, HRP shows a more even spread of risk, aligning with a diversification shift away from BTC toward other crypto assets like BCH and XLM. ENB portfolios are also more aligned in terms of weights and risk contributions, suggesting the optimization succeeds in distributing more uniformly in terms of volatility and correlation.

The MAXDIV portfolio emphasizes high-volatility, low-correlation assets such as SPXT and XRP. At both dates, we observe some disconnect between weights and risk contributions, especially at dateTr, where risk contributions are more dispersed due to rising correlations and volatility spikes. This is consistent with the method's goal to maximize the diversification ratio, not to equalize risk contributions.

The EW portfolio is instructive as a benchmark: it assigns equal weights by design, but its risk contributions are far from uniform. Assets with high volatility or strong correlation (e.g., ETH, BTC) dominate the risk profile. This clearly illustrates that naive equal weighting leads to uncontrolled risk exposures, a point that all optimized methods seek to address.

Finally, we would not feel comfortable holding the MVP or ERC portfolios at their optimal weights because they allocate nearly all capital to a single asset (SOFR), resulting in portfolios that are overly concentrated and practically uninvestable. In contrast, we are much more comfortable with the ENB, HRP, and MAXDIV portfolios. These offer meaningful diversification across assets, reflect underlying market structure, and provide more balanced exposure to risk and return. The Equal Weight portfolio is also easy to hold psychologically, though it hides significant risk concentration.

All optimizations were performed using only non-negativity (no short selling) and leverage constraints (weights sum to 1). However, the extreme concentration in MVP and ERC suggests that in a real-world setting, it would be necessary to add additional constraints, such as maximum weight caps or diversification limits, to ensure the portfolios are practical and diversified enough for actual investment.

## 4) Extensions to Hierarchical Risk Parity:

### a. Alternative HRP optimization:

In the construction of financial portfolios, one of the key challenges is to correctly model the dependencies between assets. The traditional dependence on Pearson correlation, as employed in classic risk-based approaches such as in Lopez de Prado's original Hierarchical Risk Parity (HRP) model<sup>3</sup>, has been questioned in the academic literature for its inability to capture non-linear, asymmetric or tail dependencies. This limitation is particularly strong in volatile and structurally unstable markets such as cryptocurrencies, where asset returns can exhibit extreme co-movements and regime shifts. In their article, Embrechts, McNeil and Straumann (1999)<sup>(1)</sup> and<sup>(2)</sup> warn against the unselective use of correlation coefficients, pointing out their many pitfalls, particularly in the presence of non-elliptical return distributions or in the event of market tensions. To remedy this, the authors recommend moving towards more robust measures of dependence, such as distances based on copulas and Kendall's tau, as studied by Schweizer and Wolf (1981)<sup>6</sup>. This part of the project is therefore motivated by the need to improve the HRP framework. We replace the standard correlation-based distance matrix of part 3.a)iv. with a more flexible and robust dependency measure, i.e. a copula-based approach.

And that is exactly what we implement in our code. First, we write the function "empirical\_cdf" which ensures each variable is standardized in a distribution-free way before entering the copula transformation. This function will be useful in the next part of our code. Then, the main function for this part, "copula\_kendall\_distance\_matrix" builds a dependence-based distance matrix using the Gaussian copula-implied Kendall's tau, as suggested in Schweizer and Wolf (1981)<sup>6</sup> and recommended by Embrechts, McNeil, and Straumann (1999)<sup>(1)</sup> and<sup>(2)</sup>. First, we prepare a square matrix to store Kendall's tau values between each pair of assets. Then, we apply an empirical CDF to convert returns into uniform [0,1] values (copula margins). We use "norm.ppf(.)" to transform uniforms into standard normal variables, as in the Gaussian copula model. This process standardizes all assets to a common marginal (standard normal), focusing on dependence structure only. Then we compute the Pearson correlation in the transformed space of the copula and convert that correlation into Kendall's tau using a closed-form relationship for Gaussian copulas:

$$\tau_{ij} = \frac{2}{\pi} \arcsin(\rho_{ij})$$

We convert the dependence (tau) into distance, creating the distance matrix using:

$$d_{ij} = \sqrt{0.5 \cdot (1 - \tau_{ij})}$$

And finally it returns a symmetric distance matrix of shape N×N (N = number of assets = 14), which will be used in hierarchical clustering. Finally, we create the function compute\_hrp\_alternative, which uses the same logic as compute\_hrp used in point 3.a)iv., but this time with the copula-based distance matrix.

All of these functions explained in this part are in the file "utils.py".

### b. Weights for alternative HRP:

In this section, we are going to compare the new weights we just found for the alternative HRP with those found for the classical HRP in point 3.a)iv.. In Table 8 and Figure 21, we can observe the different weights for both methods and for both dates, datePP and dateTr.

	DatePP		DateTr	
	Standard HRP PP	Alternative HRP PP	Standard HRP Tr	Alternative HRP Tr
ADA_USD	0.015810	0.039117	0.026057	0.084422
BCH_USD	0.011828	0.013134	0.124536	0.015463
BTC_USD	0.429570	0.214534	0.163084	0.026853
DOGE_USD	0.001201	0.000072	0.015833	0.006886
ETH_USD	0.026159	0.017555	0.020766	0.015427
LINK_USD	0.000000	0.009675	0.015094	0.012042
LTC_USD	0.013481	0.014970	0.125778	0.016929
MANA_USD	0.032660	0.009713	0.003251	0.010880
XLM_USD	0.004309	0.036761	0.105106	0.015493
XRP_USD	0.039602	0.011778	0.000000	0.013265
SPXT	0.113501	0.373552	0.057885	0.000015
XCMP	0.170687	0.003675	0.215328	0.058650
SOFR	0.058884	0.255464	0.117032	0.693685
VIX	0.082310	0.000000	0.010250	0.029990

Table 8: Weight comparison for Standard and Alternative HRP for both dates

In Figure 21, we can observe the same weights in a more visual way, again for datePP and dateTr.

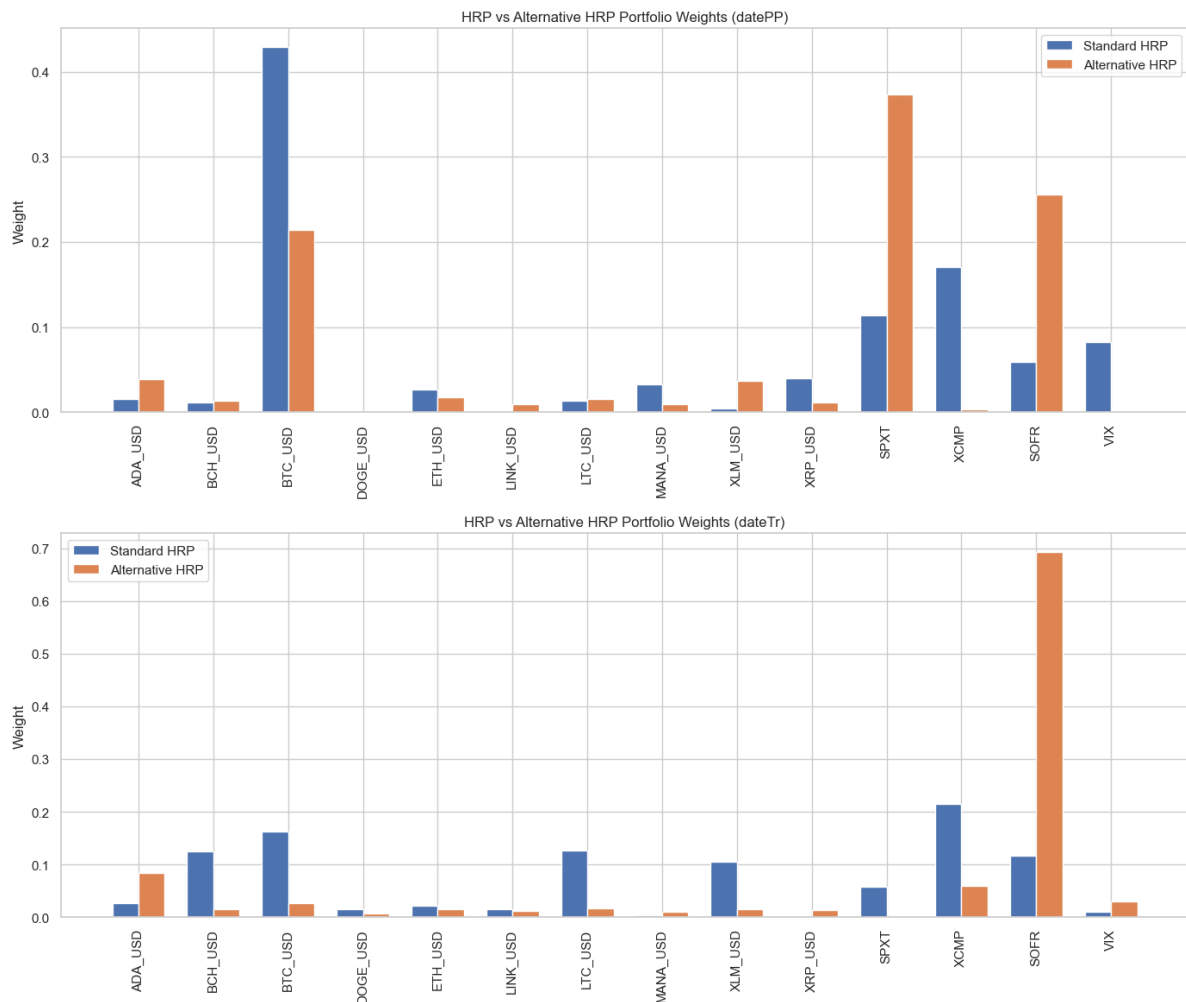


Figure 21: Weight comparison for Standard and Alternative HRP for both dates

In these two figures above, we can observe and discuss some interesting findings. First of all, at the previous market peak on September 11, 2021 (datePP), the standard HRP and the alternative HRP produced different allocations. The alternative HRP portfolio assigned a significant weight of 21.5% to Bitcoin (BTC) and over 37% to the SPXT index, whereas the standard HRP allocated almost 43% to BTC and only 11.4% to SPXT. These differences can be attributed to the distinct ways the two methods model dependence. While Pearson correlation used in standard HRP captures only linear relationships, the copula-based approach identifies stronger tail dependencies and nonlinear co-movements. It is likely that ETH and XRP exhibited a high tail correlation with other crypto assets at datePP, which the alternative HRP penalized by assigning them lower weights of 1.8% and 1.2% respectively. Conversely, BTC and SPXT were identified as structurally distinct within the dependence hierarchy, justifying their higher allocations. Although both methods allocated minimal weight to the VIX, the divergence in SPXT exposure underscores how the models perceive traditional equity indices differently under varying dependence frameworks.

At the time of the crash on November 21, 2022 (dateTr), the distinction between the two methods became even more pronounced. The alternative HRP significantly reduced total crypto exposure from around 45% at datePP to approximately 20%, distributing it pretty evenly across every cryptocurrencies. In particular, BTC's allocation decreased to 16.3% in standard HRP and to only 2.7% in alternative HRP. Instead, the alternative HRP heavily reallocated towards traditional low-risk instruments, assigning nearly 70% to the SOFR rate and 5.9% to XCMP, while SPXT was virtually eliminated from the portfolio. This suggests that SPXT's dependence structure became increasingly correlated with crypto assets in the tails during the crash, rendering it less useful as a diversifier. Meanwhile, the standard HRP showed little responsiveness to the regime change: its portfolio remained roughly the same from datePP, continuing to allocate substantial weight to crypto, and setting BTC as its largest position. This structural inertia reflects the limitations of Pearson correlation, which does not adjust effectively to evolving market dynamics.

These results confirm that copula-based HRP is more sensitive to regime shifts and better able to recognize changes in tail risk and systemic co-movements. By dynamically reassessing the structural relationships between assets, the alternative HRP is able to reduce the weighting of highly dependent groups and favor safer allocations where appropriate. Standard HRP, on the other hand, maintains its allocation logic regardless of changing market conditions, which can lead to excessive risk exposure during periods of stress.

### **c. Combining Time Series Momentum (TSM) and HRPe portfolio:**

Up to this point in the project, portfolio construction has been based only on risk-based approaches. These methods, including Equal Weighting (EW), Minimum Variance and Hierarchical Risk Parity (HRP), assume no ability to predict future returns. Their primary objective is to improve diversification and manage portfolio volatility, not to generate alpha. However, as Moskowitz, Ooi and Pedersen (2010)(4) point out, there is empirical evidence that individual assets exhibit time-series momentum (TSM), meaning that their past returns can predict future returns. In other words, assets that have performed well over the past year tend to continue to perform well, and vice versa. This paves the way for the integration of predictive signals into our portfolio strategy. Moreover, the structural robustness of our copula-based HRP (HRPe) from part 4(a), combining it with a TSM signal seems particularly promising. This approach has recently been studied by Cirulli, Kobak and Ulrych (2024)(5), who demonstrate that combining structural diversification with trend-following signals can lead to better-performing portfolios in terms of both risk-adjusted return and stability. So, in this section, we construct and evaluate a TSM + HRPe portfolio over the entire sample period, allowing long and short positions in the interval [-1,1], and compare its performance to the previous equally weighted portfolio.

So, we start by creating a function "compute\_tsm\_signals", that creates a TSM signal for each asset based on its 12-month log return, as proposed in Moskowitz et al. (2010)(4). It can assign 3 different value to each asset: If the asset's past 252-day return is positive, assign signal +1 (go long), if negative, assign -1 (go short), and if flat, assign 0 (neutral). This provides directional information for each asset based on its own historical performance, independent of others. Then, we create a function "combine\_tsm\_hrpe", that combine the two strategies by multiplying the HRP weights (structure) with TSM signals (direction). Note that the final portfolio respects the fact that the sum of the absolute weights equals one, but allows long and short positions without enforcing non-negativity. And finally, in Table 9 and in Figure 22, we can observe the different weights for this combined portfolio.

	Combined TSM + HRPe Weights
ADA_USD	0.063379
BCH_USD	-0.015028
BTC_USD	0.179937
DOGE_USD	-0.008473
ETH_USD	-0.020725
LINK_USD	0.052813
LTC_USD	0.001016
MANA_USD	-0.009224
XLM_USD	0.013561
XRP_USD	0.012834
SPXT	0.417876
XCMP	0.011939
SOFR	0.193195
VIX	-0.000001

Table 9: Weight for Combined TSM + HRPe

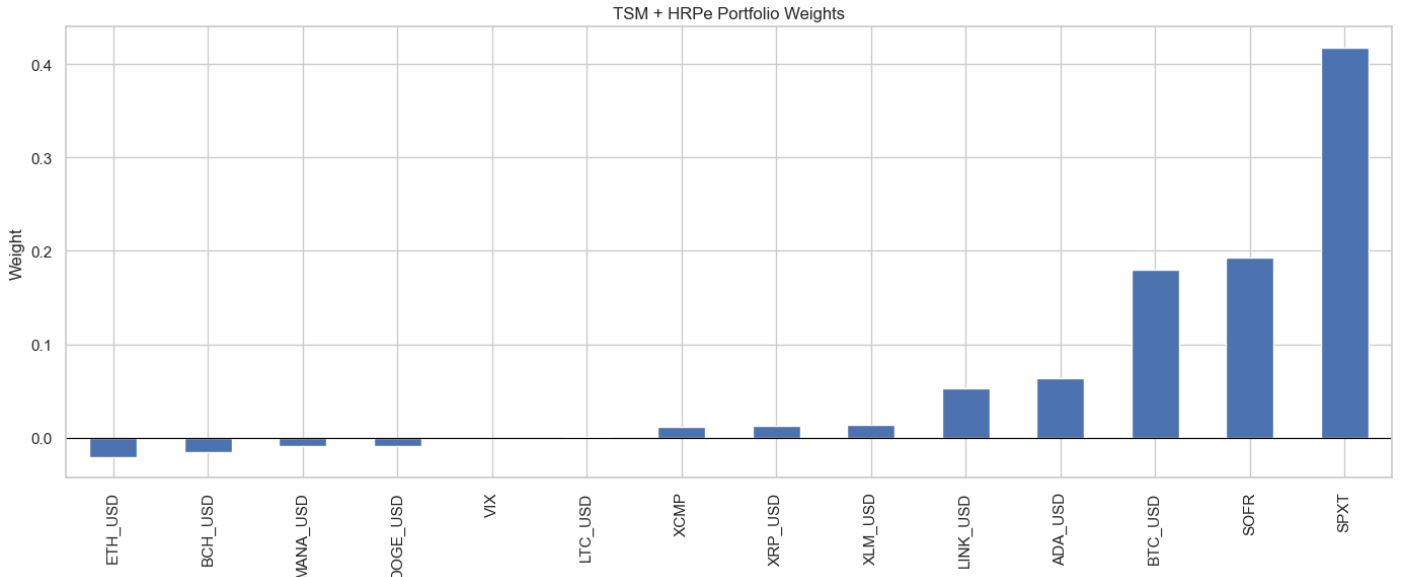


Figure 22: Weight for Combined TSM + HRPe

We can observe that we go short in ETH, BCH, MANA and DOGE, and strongly go long in BTC, SOFR and SPXT. This corresponds to our previous assertions, which imply investing in more stable (less volatility) and secure assets. Then, we compute the cumulative performance for 1\$ invested in the

TSM + HRPe portfolio over the full period (2017–2025) and is shown in the Figure 23 below.

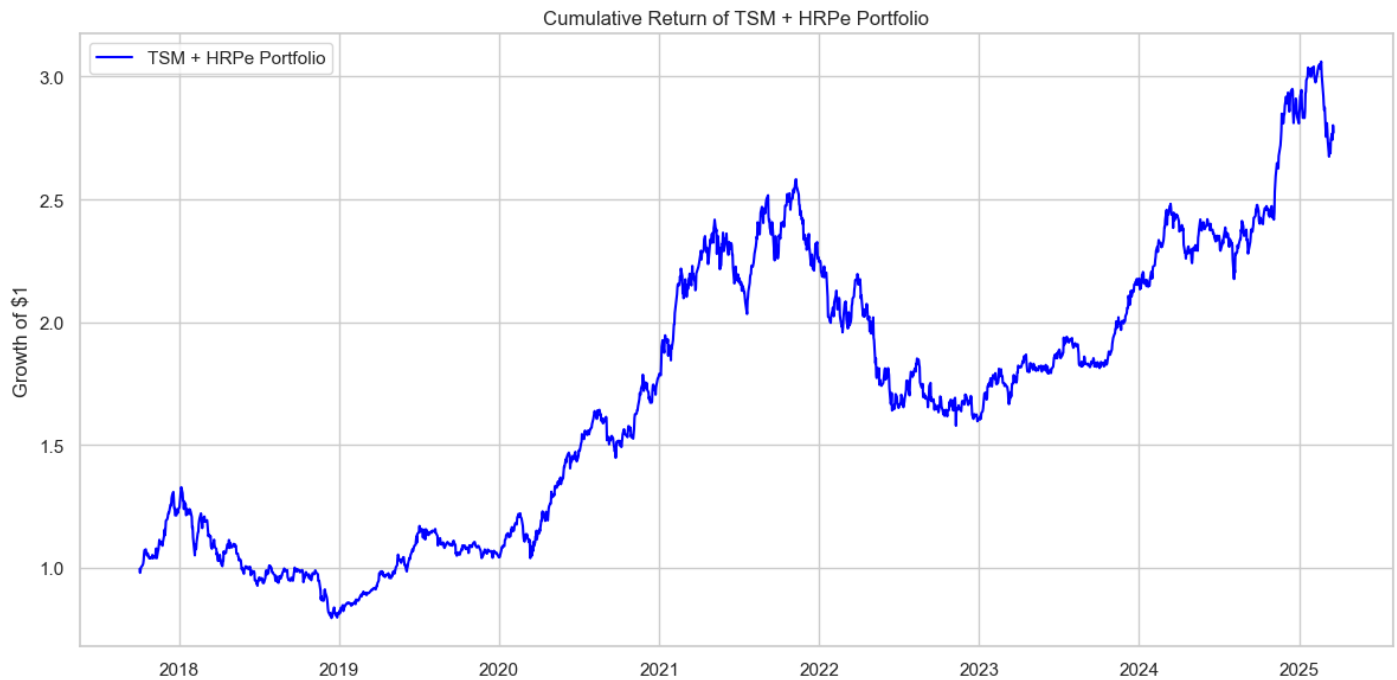


Figure 23: Cumulative Return of TSM + HRPe Portfolio

It shows a trend close the the one of the SPXT, which is normal as we have more than 40% invested in it. In order now to compare the performance of this new portfolio with the equally weighted portfolio, we then compute different performance metrics: the annual return, the annual volatility and the Sharpe ratio. We can see the results in the Table 10 below.

	Annual Return	Annual Volatility	Sharpe Ratio
Equally Weighted	0.032593	0.489234	0.066620
TSM + HRPe	0.132555	0.204158	0.649273

Table 10: Comparison of performance metrics for equally weighted and TSM + HRPe portfolios

We can observe a logically bigger annual return for the HRPe + TSM portfolio in comparison to the equally weighted portfolio, and also a way smaller annual volatility, resulting in a way bigger Sharpe ratio. To even better analyze these results, we plot the performance of both portfolios on the same graph in Figure 24.

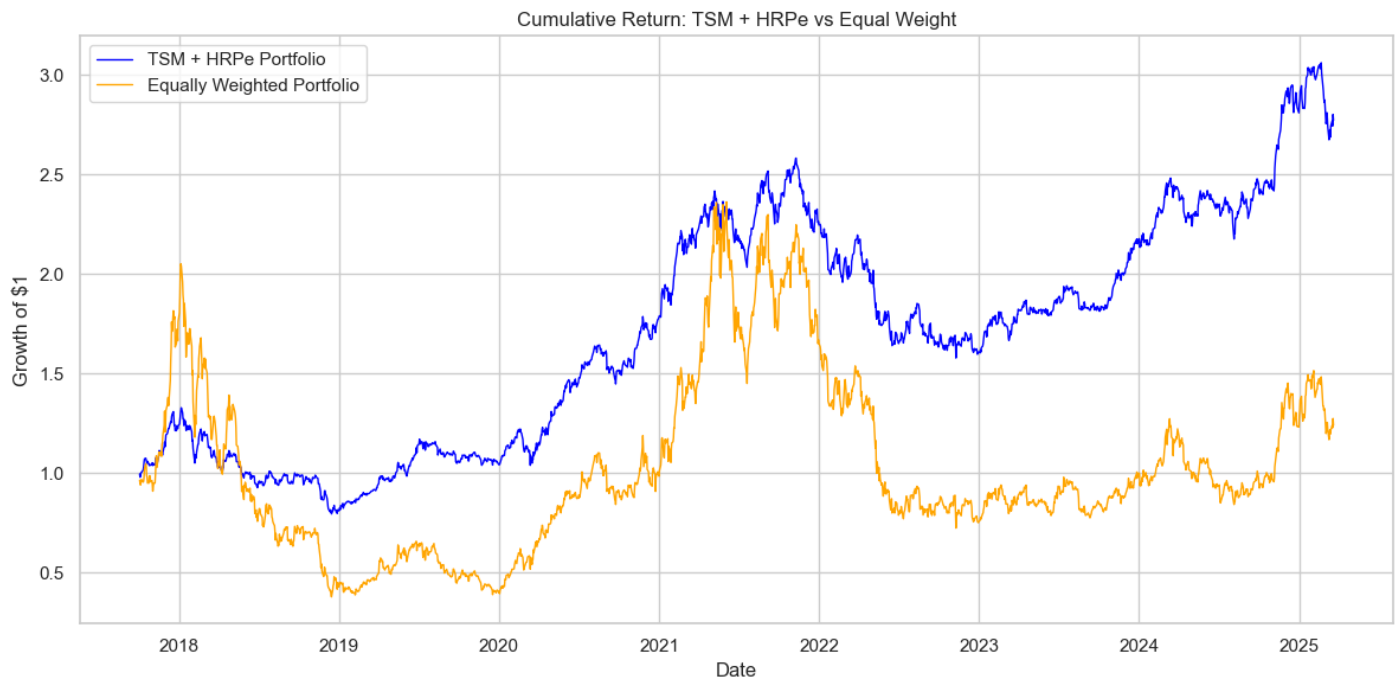


Figure 24: Performance Comparison of Equally Weighted and TSM + HRPe Portfolio

For the equally weighted portfolio, we can observe that the cumulative returns vary a lot and depends very much on the state of the economy and sometimes seems a bit random or lucky. Whereas for the combined TSM + HRPe portfolio, the cumulative performance shows a steadier and smoother growth trajectory. It appears to avoid major drawdowns more effectively and benefits from trend persistence. This means that it is much less exposed to risk than the equally weighted portfolio. This is confirmed by the annual volatility computed in Table 10. Although the equally weighted portfolio achieves, at some points, a better cumulative return, it is much riskier and exposed to the high volatility and random variations that crypto-currencies can experience than the combined TSM + HRPe portfolio. So we can confirm that there is a certain improvement by combining the two methods (TSM + HRPe) in comparison to just an equally weighted portfolio.

*Do not hesitate to consult our code if anything is unclear to you, as it is well commented.*

## Bibliography

1. Embrechts, P., McNeil, A., and Straumann, D. (1999) *Correlation and Dependence in Risk Management: Properties and Pitfalls*. Zurich: ETH Zurich.
2. Embrechts, P., McNeil, A., and Straumann, D. (1999) *Correlation: Pitfalls and Alternatives*. Zurich: ETH Zurich.
3. López de Prado, M. (2016) *Building Diversified Portfolios that Outperform Out-of-Sample*. New York: ARPM (Advanced Risk and Portfolio Management), *The Journal of Portfolio Management*.
4. Moskowitz, T.J., Ooi, Y.H., and Pedersen, L.H. (2010) *Time Series Momentum*. Amsterdam: Elsevier, *Journal of Financial Economics*, pp. 228-250.
5. Cirulli, A., Kobak, D., and Ulrych, L. (2024) *Portfolio Construction with Hierarchical Momentum*. New York: Institutional Investor Journals, *The Journal of Portfolio Management*, pp. 136-159.
6. Schweizer, B., and Wolf, E.J. (1981) *On nonparametric measures of dependence for random variables*. New York: Institute of Mathematical Statistics, *The Annals of Mathematical Statistics*.
7. Bouchaud, J.-P.; Potters, M. (2011). *Financial applications of random matrix theory*: A short review. In: *The Oxford handbook of Random Matrix Theory*. Oxford University Press. 824–850
8. Attilio Meucci (2010) *Linear vs. Compounded Returns – Common Pitfalls in Portfolio Management*. QuantNugget, [www.ssrn.com](http://www.ssrn.com).
9. Fernando Luque (2025) *These Top Income Stocks Are Europe's Dividend Aristocrats*. Morningstar.
10. Tasche, Dirk. *Euler allocation: Theory and practice*. Technical Report, 2007.
11. Higham, D. J. (1995). *Condition numbers and their condition numbers*. *Linear Algebra and its Applications*, 214, 193-213.
12. Bellalah, M., Zouari, M., Sahli, A. and Miniaoui, H., 2015. *Portfolio credit risk models and name concentration issues: Theory and simulations*. International Journal of Business, 20(2), p.111.
13. Meucci, A., 2009. Managing diversification. Risk, pp.74-79.
14. Markowitz, H. (1952). Portfolio Selection. *The Journal of Finance*, 7(1), 77–91.
15. Roncalli, T. (2009). On the properties of equally-weighted risk contributions portfolios, Available at <http://thierry-roncalli.com/download/erc.pdf>.